NASA CONTRACTOR REPORT

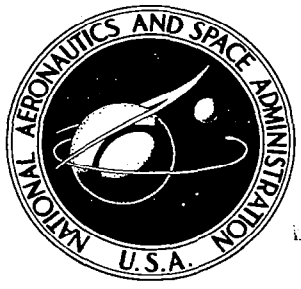

TEMPERATURE CONTROL OF THE ORBITAL OTOLITH EXPERIMENT

by Paul R. Schrantz

Prepared by
THE JOHNS HOPKINS UNIVERSITY
APPLIED PHYSICS LABORATORY
Silver Spring, Md.
for

NATIONAL AERONAUTICS AND SPACE ADMINISTRATION • WASHINGTON, D. C. • JUNE 1967

NASA CR-815

TEMPERATURE CONTROL OF THE ORBITAL OTOLITH EXPERIMENT

By Paul R. Schrantz

Issued by Originator as TG-815

Prepared under Contract NOw 62-0604-c by
THE JOHNS HOPKINS UNIVERSITY - APPLIED PHYSICS LABORATORY
Silver Spring, Md.

for

NATIONAL AERONAUTICS AND SPACE ADMINISTRATION

For sale by the Clearinghouse for Federal Scientific and Technical Information
Springfield, Virginia 22151 – CFSTI price $3.00

ABSTRACT

This report presents a description of the temperature control system which has been developed for the Orbital Otolith Experiment. The experiment has been packaged in a cylindrical vessel which will be installed in one of the first manned orbital Apollo missions. Its prime function will be to monitor the response of the vestibular nerves of two frogs under zero gravity conditions. Because of the sensitivity of these measurements, and the experimenter's desire to limit the number of variables, the water in which the frogs are to be totally submerged must be maintained at 65 ±5°F for approximately 100 hr in orbit.

The program has been funded by the Ames Research Center (NASA) and has reached the completion of the engineering model phase. A discussion of the initial thermal vacuum test results is included along with a presentation of the thermal design analysis and calculations. Information obtained in both system- and component-level tests has been implemented in the design of a flight prototype unit, which will be essentially identical to the two flight models scheduled to be supplied to NASA in the second half of 1966.

TABLE OF CONTENTS

LIST OF ILLUSTRATIONS

LIST OF SYMBOLS

q	=	total rate of heat flow, w
q'	=	rate of heat flow/unit area, w/ft^2
A	=	area, ft^2
σ	=	Stefan-Boltzman constant, 0.173×10^{-2} $Btu/(ft^2)(hr)(°R)^4$
e_1	=	total normal infrared emittance of pressure vessel coatings
e_2	=	total normal infrared emittance of internal Service Module surface in Bay I area
T	=	absolute temperature, °R
K	=	thermal conductivity, $Btu/hr\ ft^2°F/ft$
R	=	thermal resistance, °F/w
ℓ	=	length of thermal insulators
W	=	weight, lb_f
C	=	specific heat, Btu/lb_f
t	=	time, hr
F_e	=	emittance coefficient
U	=	overall atmospheric heat transfer coefficient, $w/ft^2°F$
h_c	=	free convection heat transfer coefficient, $Btu/hr\ ft^2°F$

I. INTRODUCTION

The study of weightlessness has become a vital subject in man's advance toward orbital and lunar flight. One particular aspect of this subject (the effect on the otoliths, which are contained in the vestibular nerve) is currently being investigated by Dr. T. Gualtierotti, an Italian scientist on loan to the Ames Research Center. A major step in the completion of his study will be the results obtained from the orbital flight of two frogs. Nerve signals and electrocardiograms (EKGs) will be monitored on a regular schedule during the 100-plus hours of the flight. During each monitoring period, a fixed level of artificial gravity will be imposed for a short time by a centrifuging technique. In January 1965, NASA decided to include the experiment on one of the first manned Apollo orbital missions. With these objectives in mind and under NASA funding, APL has designed, built, and tested an engineering model of an experimental capsule. A flight prototype is scheduled for completion and testing in the near future, and two flight models are to be supplied to NASA in the second half of 1966.

The basic APL system is made up of an inner assembly, which includes a cylindrical container for the two frogs along with a complete life-support system, and an outer cylindrical vessel which will maintain approximately 7.5 psia internal pressure. The cylinder housing the two frogs has its axis perpendicular to that of the outer structure. The upper and lower bulkheads of the inner assembly contain bearings and a drive system which permit the cylinder to be spun to produce artificial gravity. In the early design stages, a decision was made to use a General

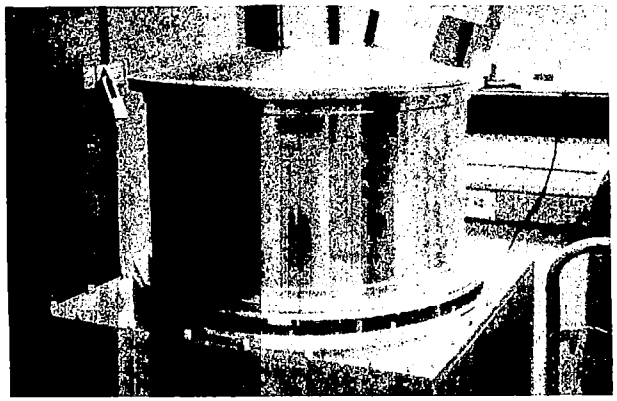

Fig. 1 PRESSURE VESSEL, EXTERNAL VIEW

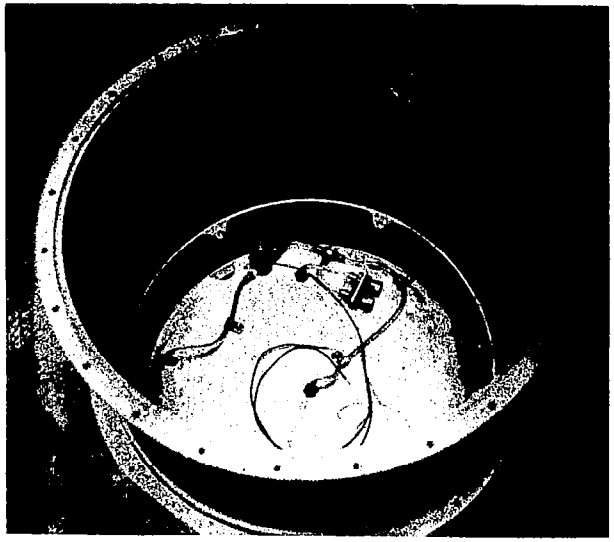

Fig. 2 PRESSURE VESSEL, INTERNAL VIEW

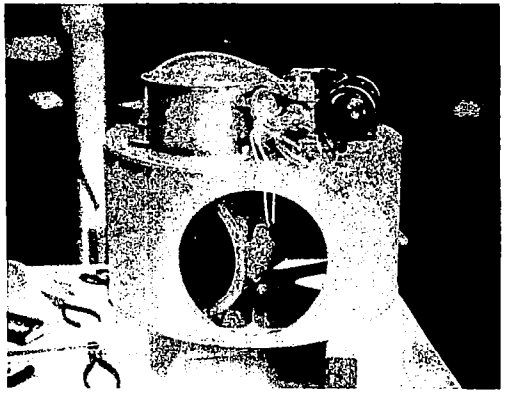

Fig. 3 INVERTED INNER ASSEMBLY, SIDE VIEW

Fig. 4 INNER ASSEMBLY, BOTTOM VIEW

Electric perm-selective membrane in order to permit total submergence of the frogs for the duration of the mission. By means of this "lung," it is possible to supply O_2 to the circulating water and remove the CO_2 generated by the frogs. Removal of the CO_2 is accomplished by circulation of the gas through a barylime cannister. Circulation of the water and O_2 is carried out by means of a small pump and a blower, which are driven by brushless DC motors. Experimental signals are amplified on the rotating cylinder and passed through slip rings to a signal plug mounted on the pressure vessel. The experiment is supplied with 28-v DC from the fuel cells which make up the Apollo mission power system. Several photographs are shown in Figs. 1, 2, 3, and 4. As a matter of reference, the outer vessel is seen mounted on a flange (Fig. 1) which is located about midway along its length. Its overall length is approximately 20 in., and it is approximately 16 in. in diameter.

Although the experiment will be exposed to the vacuum of outer space, the shell will see only the internal structure of the service module of the launch vehicle. Information on the expected temperature environment of the structure has been obtained from the vehicle contractor, North American Aviation Inc., Space and Information Systems Division, Downey, Calif. (NAA). Since it has been necessary to set the thermal design without benefit of a mission profile, it is obvious that the best solution to the temperature control problem is to attempt to isolate the experiment from the launch vehicle with respect to heat flow, and to provide a self-contained method of cooling. In this particular case, cooling is of prime importance since there must be a way of dissipating the heat generated by the life-support equipment and of covering those times when the service module ambient is significantly higher than the control temperature.

Another condition must be considered in the thermal design concept. The experiment will be mounted in the vehicle about 6 to 12 hr prior to launch. During this time, care must be taken to prevent the temperature of the life-support water from rising above the upper control limit prior to lift-off. Here there are the added effects of convection and of decreased efficiency of the high vacuum insulation employed in the launch vehicle. The control concept during the pre-launch phase will be discussed in detail in a later section.

II. THERMAL ENVIRONMENT

The manned Apollo orbital vehicle is made up of two stages. The prime stage is the Command Module in which the three astronauts are stationed; the other is the Service Module (SM) in which fuel cells, life support tanks, propulsion systems, etc. are located. The Orbital Otolith Experiment will be mounted in a hole in a structural shelf at approximately Station 277 of the Service Module. Figures 5 and 6 show sketches of the shelf and surrounding structure.

At a meeting in Downey, California, on 28 January 1965, NAA provided information on the structure's temperature limits in the area of the mounting hole. This information was outlined in a preliminary design review (Ref. 1). APL requested clarification of these data, and the updated results were forwarded in August 1965 (Ref. 2), and are summarized below. Temperatures given are the worst cases, hot and cold, to be experienced during the mission.

Temperature Limits for Structure

Mission Event	Shelf Temp., °F		Surrounding Temp., °F	
	Max.	Min.	Max.	Min.
Pre-launch (T-7 hr to launch)	91	60	90	60
Launch	See Fig. 7		120	80
Earth orbit	See Fig. 7		80	40

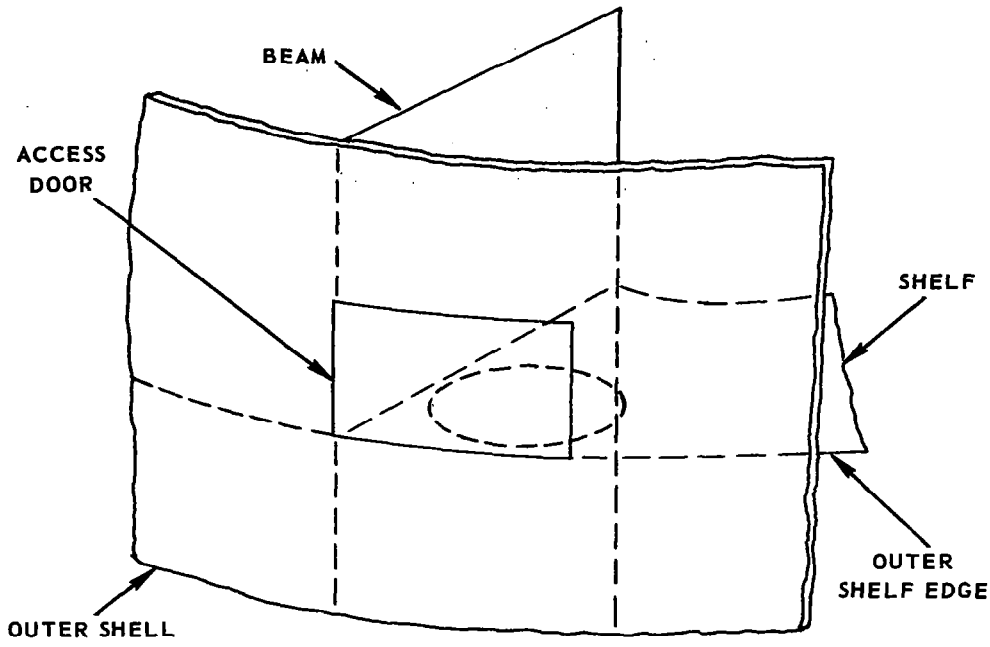

Fig. 5 SERVICE MODULE, BAY I, STATION 277

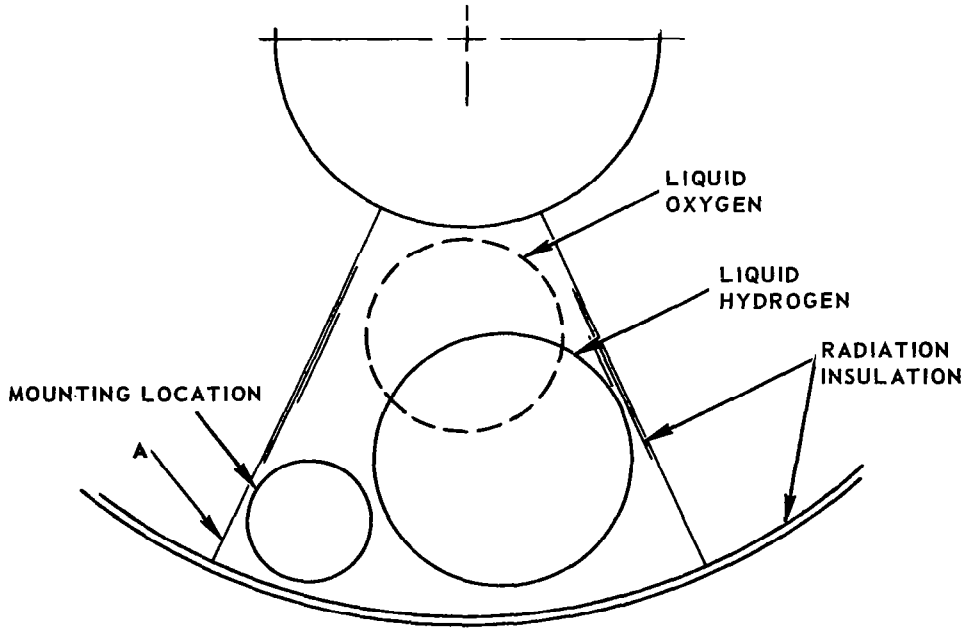

Fig. 6 TOP VIEW, BAY I, STATION 277

In this table, temperatures are defined as follows:

Shelf temperature adjacent to access hole--average around hole

Average surrounding temperature--during pre-launch phase, applies to adjacent SM structure, and to the near-stagnant air in Bay 1. During spaceflight, the temperature applies only to the adjacent structure. The emittance of the structure is given as 0.25.

A brief description of the mission events will now be given to shed further light on the thermal design problem. At this date, there has been no final decision as to what time in the pre-launch schedule the experiment will be mounted on the shelf and the access door installed. The NAA information indicates that the temperature of the surroundings could reach 90°F at some time during the seven hours before launch. As a result, it was decided to assume that the maximum temperature condition will exist during the entire pre-launch period. This represents a conservative approach to the pre-launch control problem.

It can be seen (Fig. 7) that, although the peak launch temperatures are quite high, their duration is relatively short. NAA has indicated that the surrounding structural temperatures will follow the rise and decay pattern shown for the shelf. The orbital temperature control system (evaporator) becomes operative as soon as vacuum conditions are reached. Thus the launch event is perhaps the least troublesome problem.

The earth orbit data are given in rather general terms, because there has been no definition of vehicle orientation for the entire mission,

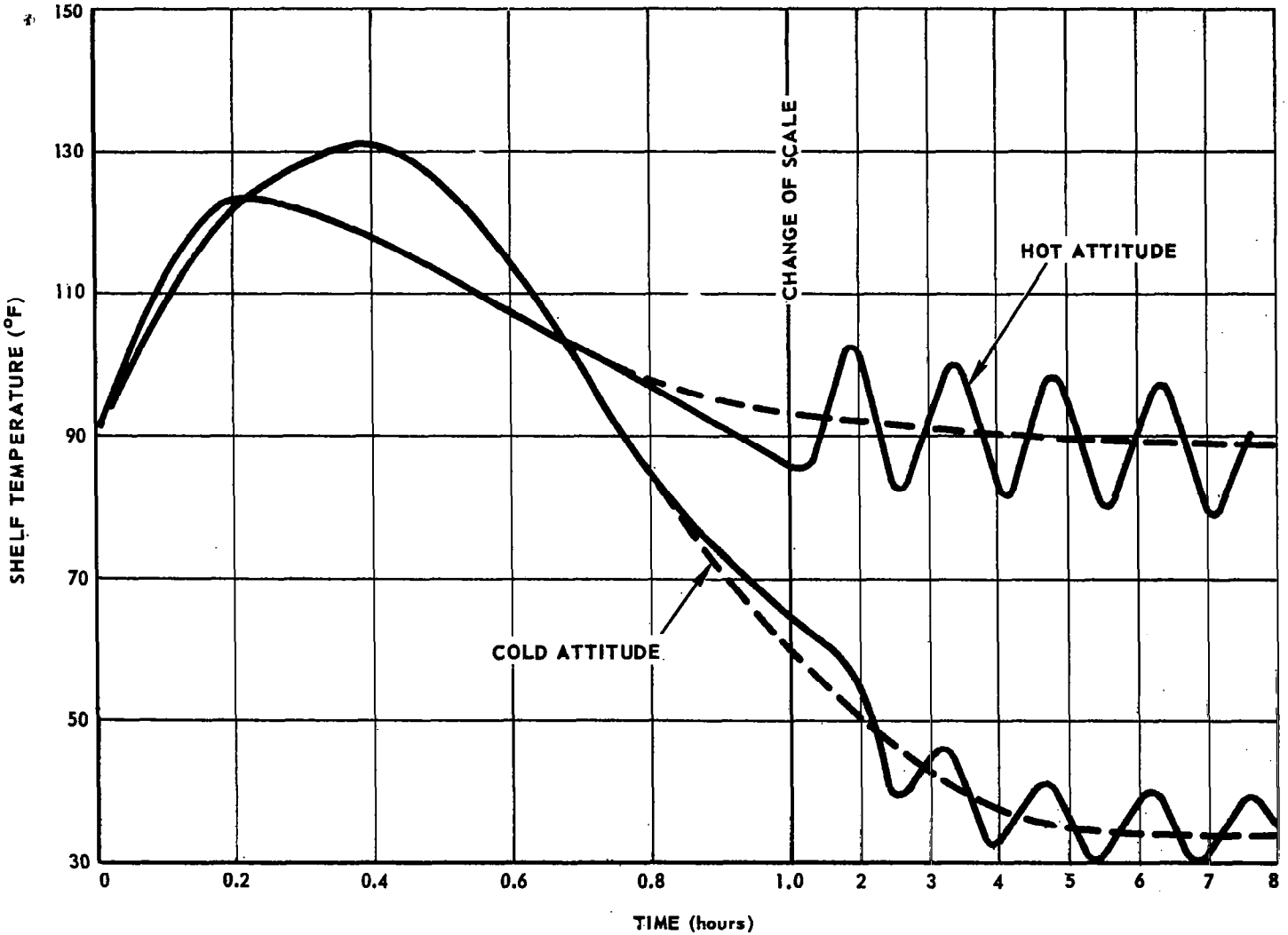

Fig. 7 TEMPERATURE HISTORIES OF THE SHELF

to date. The maximum and minimum temperature limits given are probably for cases where Bay 1 faces directly towards the sun and away from the sun, respectively. Although it is unlikely that the entire mission could be spent at these orientations, it was decided that the temperature control system should be capable of handling these steady state cases for undetermined lengths of time. Control accuracy, therefore, should not diminish with time.

III. COOLING SYSTEM--REQUIREMENTS AND SELECTION

It was stated earlier that, in an attempt to minimize the number of variables in the experimental system, the experimenter has required that temperature of the life-support water be maintained within relatively close tolerances. Although a temperature limit of 60°F (+10°, -5°) was originally imposed, this was later changed to 70 ±5°F. After a series of temperature-controlled life-support tests at APL in August 1965, a final limit of 65 ±5°F was agreed upon.

It will be shown that the steady state condition of minimum ambient structural temperatures can be handled passively by proper isolation of the experiment. The term "isolation" is used here to indicate that heat exchange between the experiment and the Service Module is minimized by use of insulation at the mounting flange, and control of the emittance of the external pressure vessel coating. During this mode of operation, the internal dissipation of heat from electrical equipment in the life-support system is helpful in maintaining the desired control temperature.

During periods when maximum ambient temperatures are experienced, however, the picture is different. Original calculations indicate that a temperature rise of 3°/hr would occur under normal operating conditions with optimum thermal isolation of the experiment. At this rate, the upper temperature limit would be exceeded in less than five hours. Since there is no definition of the length of time which might be spent at the maximum structural ambient, it is obvious that an active cooling capability is required to guarantee adequate temperature control.

In the initial phases of the design, three separate cooling techniques were considered. They were:

1. Thermoelectricity
2. Cold gas expansion
3. Evaporation

It appeared that the cooling required to meet the initial NAA temperature limits could be achieved by the use of a number of thermoelectric modules (Ref. 1). Although this technique offered the distinct advantages of minimum size, weight, and mechanical development, it became obvious that it would be difficult to achieve adequate control margins.

During a telephone conversation with D. Maize of NAA (Ref. 3), it was noted that a tolerance of ±15°F should be placed on original temperature limits. An APL analytical study of the heat sink capability of the honeycomb shelf indicated that the thermal resistance offered by the 0.016 aluminum faces resulted in a relatively high temperature buildup at the locations where heat was to be transferred. Although this problem could have been handled by a Service Module modification, it was agreed that this approach would be expensive and impractical. With the increased temperature difference, the coefficient of performance of the thermoelectric modules would be substantially reduced, with a resulting increase in the electrical power requirement.

It was therefore decided that the other two cooling techniques should be reconsidered. Although it was possible to employ the desired degree of thermal isolation with a cold gas expansion system, calculations indicated that a net cooling effect of only about 70 Btu/lb could be

realized. The weight and packaging limitations were obvious. The high heat of vaporization of water (1000 Btu/lb) seemed to eliminate these problems. Initial calculations indicated that about 10 pounds of water would be necessary and that sufficient storage space was available (290 in^3). Because of the close fit of the pressure vessel in the hole in the Service Module shelf, it was decided that the evaporator should be located on the lower end of the vessel. As the design of an engineering model of the evaporator was being completed, a prototype evaporator was built and tested. These tests indicated that evaporative cooling could be successfully employed in the thermal design of the Orbital Otolith Experiment. One drawback to this system had to be overcome. The evaporator functions only under vacuum conditions, and hence is inoperable during the pre-launch phase. This disadvantage is not quite as serious as it appears to be. The evaporator water supply provides additional thermal inertia to the system. Any chilling of this supply below the control temperature can be used as a passive cooling technique during the pre-launch phase. This effect will be discussed in detail in a later section.

IV. THE THERMAL CONTROL SYSTEM

Thermal control for the orbital phase of the experiment is achieved by the following:

1. Minimization of radiative heat leakage to and from the Service Module by the selection of a low emittance external coating for the pressure vessel
2. Reduction in conductive heat leakage at the mounting flange resulting from the use of 14 rubber vibration mounts (good thermal insulators)
3. Provision of active open-system cooling of the outer shell by a water evaporator
4. On-and-off control of evaporator water supply by means of a thermostat in the life-support water circuit
5. A heat exchange unit built into the lower bulkhead of the inner assembly to transfer heat to and from the water
6. Minimization of thermal resistance between heat exchanger and evaporation inlet location to produce maximum cooling effect

In the next section of this report, calculations will be presented to show how this approach was carried out.

Under normal operation, the evaporator water flow is controlled by a timing circuit which opens and closes a solenoid valve. The water supply is contained in a bladder so that the 7.5 psia internal pressure

can be used to provide the necessary differential for flow. When the thermostat senses a temperature above the nominal control temperature (65°F), water flows into the evaporator. A relief valve maintains a pressure of 3 in. of water in the evaporator. At this pressure, the water expands to a mist at approximately 37°F. Upon impinging on the surfaces in the evaporator, the water droplets boil while extracting a large percentage of the heat of vaporization from the aft portion of the pressure vessel. As the temperature of the outer shell decreases, a gradient is set up between the shell and the lower bulkhead, primarily in the region of the heat exchanger. With the gradient established, heat is removed from the circulating water. It should be noted that some convective cooling will take place within the vessel, but this effect will be at best minimal under zero gravity conditions. Thus the system is designed to provide the necessary cooling by conduction alone. When the water temperature decreases, the thermostat shuts off the solenoid. Because of the thermal inertia of the system, the temperature of the circulating water continues to drop for a certain length of time. The system then gradually heats up because of the internal heat load and heat leakage from the outside, until the water temperature again exceeds the thermostat value. The cycle is then repeated.

Thermal vacuum test results, determined for conditions where maximum ambient temperatures are experienced, show that this duty cycle may result in "off" times as long as three hours. In the flight design it is felt that the "on" time can be reduced to as short as 30 min by elimination of some of the minor problems which developed in the engineering model. For the conditions when maximum ambient temperatures are experienced, internal heat dissipation and external

leakage add up to about 20 watts. As the structural ambient temperature decreases, the net heating effect decreases also, so that the evaporator may not be needed at all. Prior to reaching these low temperatures, much longer "off" times will obviously be experienced.

During conditions when minimum ambient temperatures are experienced, it has been stated that the internal dissipation is used to maintain the water temperature above the negative tolerance value. This is possible since the heat leakage is maintained at a level below the internal dissipation value.

The previous description applied to the orbital phase of the mission. Although this phase covers a major portion of the total mission time, thermal control during the pre-launch and launch phases are also of importance. The data obtained during the transition from normal gravity, through the 6-g acceleration imposed by the launch, to zero gravity are considered of utmost importance to the experimenter. Thermal control during these phases is achieved by the following:

1. Minimization of radiative and conductive heat leakage by methods previously outlined
2. Refrigeration of evaporator water supply
3. Refrigeration of pressure vessel before assembly of system
4. Refrigeration of life-support water supply to about 55°F before final assembly
5. Thermal insulation of pressure vessel above mounting flange and on evaporator pan (dependent on empirical evaluation of convective heat transfer coefficient using thermal vacuum test data)

It was previously stated that the evaporator does not function under atmospheric pressure. In addition to this, convective as well as radiative heating of the pressure vessel will result when the ambient temperature of the Service Module exceeds the temperature of the pressure vessel shell. If it is conservatively assumed that the experiment will be exposed to this temperature for seven hours, it can be seen that some method of cooling must be provided. Freon could be used at atmospheric pressure, but the amount of coolant required would be high because of the relatively low latent heats available (50 to 85 Btu/lb). In addition to this, the reaction between Freon and water in the presence of aluminum (Ref. 4) would require the development of a completely separate atmospheric evaporator.

A passive means of thermal control is available and can be employed to insure that the temperature of the life-support water does not reach the control temperature limit (70°F) during the pre-launch phase. With an aluminum shell weighing approximately 30 lb and 10.5 lb of evaporator water, it is possible to provide for a large portion of the cooling required by pre-chilling this assembly down to 50°F. In addition, permission has been obtained from Dr. Gualtierotti to refrigerate the 15 lb of life-support water supply to 55°F before final assembly of the experiment. It should be noted that the exact values of the refrigeration temperatures are a function of the two periods shown below:

t_1 = time from start of final assembly to installation in the vehicle.

t_2 = exact time period from the time of installation to lift-off.

It is felt at this time that t_1 can be held to a reasonably short time, < 1 hr, and thus the system will be able to withstand t_2 > 7 hr.

If the temperature of the life-support system exceeds 65°F before lift-off, there will be no flow of evaporator water, since flow is dependent on the pressure differential established between the pressure vessel (7.5 psia) and the evaporator (3 in. of water). However, evaporation will take place as soon as a vacuum is reached. Although it would be advantageous from the standpoint of water consumption to get through the launch phase before the evaporator is turned on, the duration of the launch phase is relatively short and can be handled without difficulty.

V. THERMAL ANALYSIS AND DESIGN CALCULATIONS

An attempt will now be made to summarize the thermal design analysis and to present some of the essential calculations that were made as a result of the analysis. The launch vehicle temperatures used in these calculations include a 10°F safety factor which is called for in the environmental test specification (Ref. 5). Where possible, the relative margin provided by this pad will be indicated.

1. Heat Leakage by Radiation--Orbital Case

Since the pressure vessel is totally enclosed in the Service Module, a radiation interchange calculation given in Eckert and Drake (Ref. 6) can be employed as a conservative approximation to the heat leakage under orbital conditions. The equation applies to concentric spheres as well as cylinders.

$$q_{net} = q_1 A_1 = F_e \sigma A_1 \left(T_1^4 - T_2^4\right) \tag{1}$$

$$F_e = \frac{1}{\frac{1}{e_1} + \left(A_1/A_2\right)\left(\left(\frac{1}{e_2}\right) - 1\right)} \tag{2}$$

Where: q_{net} = net radiative heat transfer

q_1 = radiative heat transfer/unit area

A_1 = surface area of pressure vessel

σ = Stefan-Boltzman constant

T_1 = average temperature of pressure vessel

e_1 = total normal emittance of pressure vessel at T_1

A_2, T_2, e_2 = Service Module parameters

In order to apply these equations, the following assumptions have been made:

1. The temperature of the pressure vessel is constant over its surface
2. The temperature and emittance of the Service Module surfaces are uniform
3. The area ratio is small enough that the $\left(A_1/A_2\right)\left(\left(\frac{1}{e_2}\right)-1\right)$ term can be neglected $(A_1/A_2 << 1)$

In Equation 1, the Service Module parameters have the following values:

$$30° \leq T_2 \leq 90°F$$

$$e_2 = 25$$

The probable range of the pressure vessel temperature from the time the evaporator shuts off until it is turned on again is as follows:

$$55° \leq T_1 \leq 70°F$$

The only remaining unknown on the right-hand side of Eq. 1 is e_1. It is obvious that in order to minimize q_1A_1, the emittance e_1 must also be minimized. Data on coatings were reviewed, and it was decided that polished nickel plating was the most practical solution. In addition to having a low emittance value, the coating is more rugged and less subject to corrosion than is polished silver.

Although it is likely that an emittance as low as 0.05 might be achieved (Refs. 7, 8, 9) a conservative value will be assumed to provide

for difficulties which might arise in plating or polishing. The resulting heat leakage values are tabulated below, based on $e_1 = 0.10$

Condition	T_1	T_2	qA_1
A	55°	90°	-9.0 w
B	70°	90°	-8.1 w
C	55°	30°	+5.6 w

Notes: A = max. structural ambient condition, evaporator on

B = max. structural ambient, evaporator off

C = min. structural ambient, evaporator off

A positive number indicates heat loss

A negative number indicates heat gain

If the actual $e_1 = 0.05$, the heat leakage values will be reduced by a factor of 2.0.

Margin for Condition A,

$$\frac{(qA_1)_{90°}}{(qA_1)_{80°}} = 1.4$$

2. Heat Leakage by Conduction

The experiment is mounted in a hole in the Service Module shelf and is supported on 14 cylindrical rubber mounts which provide vibration isolation from the launch environment. These mounts also provide the considerable degree of thermal isolation which is required by the thermal design concept. The calculation of heat leakage by conduction follows.

Assumptions:

1. The joint resistances provided by the shock mount rings are conservatively neglected
2. Two aluminum rings are not considered to be in the heat path
3. Temperature is assumed to be uniform around the shelf hole and also around the mounting flange

$$q' = \frac{\Delta T}{R} = \frac{T_1 - T_3}{R} \qquad (3)$$

Where: $R = \frac{\ell}{KA}$ = thermal resistance

ℓ = length of cylinders

K = thermal conductivity of cylinder material

A = total area of 14 cylinders

T_3 = avg. shelf temperature

Given: ℓ = 0.688 in = 0.051 ft

$A = 14 (\frac{\pi}{4} d^2) = 0.030 \text{ ft}^2$ for d = 0.625 in

K = 0.1 Btu/hr ft^2 °F/ft

The insulating material is BTR rubber produced by the Lord Mfg. Co., Erie, Pa.

R = 19 °F/Btu/hr = 65°F/watt

Condition	T_1	T_3	q
A	55°	98°	-0.68 w
B	70°	98°	-0.43 w
C	55°	23°	+0.49 w

Notes:

Margin for Condition A, $\frac{q_{98°}}{q_{88°}} = 1.36$

A positive number indicates heat loss

A negative number indicates heat gain

3. Internal Heat Load

The internal heat load is derived from three basic sources--the metabolic rates of the two frogs, the heat of reaction in the CO_2 absorber, and the continuous electrical power dissipated by the life-support system. Conservative values for these loads are listed below:

1. $q_{frogs} = 1$ w
2. $q_{absorber} = 0.5$ w
3. $q_{electrical} = 10.5$ w
   (a) pump = 150 ma at 28v
   (b) blower = 150 ma at 28v
   (c) electronics = << 1 w
   (d) solenoid = 75 ma at 28v

Note: The solenoid is controlled by a timing circuit in order to allow adjustment of evaporator flow rate. Power dissipation is a

function of the solenoid "on" time load and of the timer continuous load. The value shown above is that which has been derived for 5 cc/min flow rate.

Thus, the total internal heat load for the engineering model is 12 watts. Final values for the electric power dissipation will probably be somewhat lower than shown above. Any changes will be reviewed to ensure that the margins arrived at in the design phase are not seriously compromised.

4. Thermal Inertia of the System

The term "thermal inertia" is used here to describe the heat capacity of the system elements. To allow the use of specific heat values found in engineering tables, weight units are used instead of mass units. These thermal inertia values will be used in later calculations to determine response of the system during different phases of the mission. Calculated values for individual components are shown below, along with the total inertia of the otolith experiment system.

Item	Mtl.	W (lb)	C (Btu/lb °F)	W x C
Outer shell	Al	29	0.23	6.7
Inner structure*	Al	27	0.23	6.2
Centrifuge assembly	Al	4.5	0.23	1.0
Life-support water	H_2O	15	1.0	15.0
Evaporator water	H_2O	10.8	1.0	10.8
TOTAL	--	86.3	--	39.7

$(WC)_{total} = 39.7$ Btu/°F

*This item includes the weight of the pumps, motors, lung, etc. The differences in material are assumed negligible.

The system functions as three separate, but thermally connected, items. These include: (a) the combination of outer shell and evaporator water supply, (b) the inner structure, and (c) the centrifuge assembly including the life-support water supply. The first item varies with the consumption of evaporated water. Since vehicle attitude has not been defined as yet, the value of this inertia term at any given time is an unknown. To overcome this lack of information, the evaporator water flow rate has been adjusted to provide adequate cooling even if the entire orbital mission is spent under maximum ambient temperature conditions. Thus, it is possible to write the following expression for minimum effective thermal inertia of the evaporator water supply.

$$\left(W_e C_e\right)_{min.} = 0.108\,[100-t] \qquad (4)$$

t = time from launch,

Therefore: $W_a C_a = 6.7 + 0.108\,[100-t]$ (5)

and $W_b C_b = 6.2$

$W_c C_c = 16.0$

5. Evaporator Water Supply Requirements

Without belaboring the point, the exact quantity of cooling water required cannot be determined at the present time. A value can be calculated based on the assumption used to derive Eq. 4. Original calculations were made in May 1965 in order to determine whether or not the volume available in the aft section of the pressure vessel was large enough to store the required cooling water. At that time, the expected internal load was considerably higher because the design included the

use of AC motors and an inverter. Given a total heat load of nearly 30 watts, it was found that the 290 in^3 available would be adequate, providing that a highly efficient evaporator could be developed. Since it was quite unlikely that the entire mission would be spent at the maximum ambient condition, the 290 in^3 was approved.

Because of a change from AC to DC motors, and the resulting deletion of a power-consuming inverter, the total heat load has been reduced to the value shown below. It should be noted that the average continuous load of the solenoid has been conservatively included.

$$q_{tot} = q_{leakage} + q_{internal} = 21 \text{ w}$$
$$= 72 \text{ Btu/hr}$$

The total cooling capacity required is equal to the product of q_{tot} and the duration of the post-launch phase of the mission.

Given: $t = 100$ hr

$Q = q_{tot} t = 7200$ Btu

The weight of water required to provide the cooling is equal to this quantity divided by the effective cooling rate of the evaporator. Ideally, the rate will be shown to be about 1000 Btu/lb. In practice, this value is lowered by a number of factors which will be discussed later.

$$W'_{ideal} = \frac{7200 \text{ Btu}}{1000 \text{ Btu/lb}} = 7.2 \text{ lb } H_2O$$

But $290 \text{ in}^3 \ H_2O \approx 10.8$ lb

It is apparent that adequate cooling will be available for the entire mission if the evaporator efficiency is kept above the ratio of these two weights.

$$\eta_e = \frac{7.2}{10.8} = 66\%$$

It will be shown later that $\eta_e > 66\%$ has been achieved, but it has been recommended that the 10.8 lb supply be retained in order to provide an additional margin in the overall thermal design.

6. Evaporator Flow Rate

In the previous section, the total cooling capacity of the water supply was determined. Although it would be possible to derive a flow rate on the basis of the calculated thermal load, several other factors must be considered. These factors are listed below.

1. The system should be capable of lowering temperatures in the event of an overshoot due to unforeseen causes (extended launch pad hold, excessive structural temperatures, etc.).
2. The thermal lag should be minimized to prevent excessive overshoot of thermostat temperature.
3. A low "on" to "off" time ratio provides for lower electric power consumption.
4. In the area of extremely low fluid flow rates, better accuracy can be achieved with higher rates.
5. The rate should not become great enough to reduce evaporator efficiency below the minimum value.

With these factors in mind, a flow rate of 5 cc/min was selected for the engineering model system. The calculations used in determining this value are shown below.

$$f_{min.} = \frac{72 \text{ Btu/hr}}{1000 \text{ Btu/lb}} \frac{454 \text{ cc}}{\text{lb}} \frac{1 \text{ hr}}{60 \text{ min}} = 0.55 \text{ cc/min}$$

Given: $(\eta_e)_{min.} = 66\%$, where $(\eta_e)_{min.}$ = minimum acceptable evaporator efficiency

$$f_{min.} = \frac{0.55}{0.66} = 0.80 \text{ cc/min}$$

The next step in the calculation has no single answer. In considering Items 3 and 4 listed previously, it can be shown that if a flow rate of 5 cc/min is employed, an on-off time ratio of approximately 1/6 can be achieved, and the percentage error resulting from a 0.2 cc/min flow rate change is reduced from 25% to 4%. It can be shown that this rate also satisfies the conditions stated in Items 1 and 2.

$$(WC)_{tot} = 39.7 \text{ Btu/°F}$$

Since 0.8 cc/min is necessary to overcome the heat load, the additional flow can be used to drop the system temperature at the following rate:

$$Q_{net} = (4.2 \text{ cc/min})(0.66)(1000 \text{ Btu/lb}) \frac{1 \text{ lb}}{454 \text{ cc } H_2O} \frac{60 \text{ min}}{\text{hr}}$$

$$= -360 \text{ Btu/hr}$$

$$\Delta T/\text{hr} = \frac{Q_{net}}{(WC)_{tot}}$$

$$= -9°\text{F/hr}$$

Although this number shows the overall capability of the system, a more meaningful term is the rate at which the outer shell will cool down. The limits on this rate are shown below.

$$(W_a C_a)_{initial} = 17.5 \qquad t = 0$$

$$(W_a C_a)_{final} = 6.7 \qquad t = 100 \text{ hr}$$

$$Q_{tot} = (5 \text{ cc/min})(0.65)(1000 \text{ Btu/lb}) \frac{1 \text{ lb}}{454 \text{ cc}} \frac{60 \text{ min}}{\text{hr}}$$

$$= -430 \text{ Btu/hr}$$

$$\left(\frac{\Delta T}{hr}\right)_{initial} = \frac{430}{17.5} = -24°\text{F/hr}$$

$$\left(\frac{\Delta T}{hr}\right)_{final} = \frac{430}{6.7} = -64°\text{F/hr}$$

These figures give an indication of the self-compensating effect of the reduction in thermal inertia of the shell. Toward the end of the mission, the heat load will result in higher temperature rise rates, but as shown above the response of the evaporative cooler will overcome this effect. As a result of these considerations, a flow rate of 5 cc/min will be provided. Because of the flexibility of the timing circuit, the final flow rate of the flight prototype may be adjusted to reflect the actual internal loads as well as any refinements in the thermal environment information, etc.

7. Minimum Temperature--Cold Case

The active control system will maintain the water temperature near 65°F during the times when high ambient structural temperatures are experienced. When the minimum ambient structural temperature

condition is experienced, the heat leakage becomes a heat loss. The minimum average temperature is determined by equating the heat loss with the internal dissipation. A calculation can be made to show that this temperature will be higher than the minimum allowable temperature. The assumptions made in carrying out the calculations are shown below.

1. The internal heat load is minimized to reflect the most optimistic estimate of power consumption. The metabolic and CO_2 absorber loads are neglected
2. The heat load is distributed in such a way that the outer shell is at some constant temperature

$$q_{loss} = A_1 \sigma_1 e_1 \left(T_1^4 - T_2^4 \right)$$

T_1 = shell temperature

Given: $T_2 = 30°F$

$q_{frogs} + q_{absorber} = 0$

$q_{electrical} = 7.3$ w

$q_{internal} = 7.3$ w

From this, $T_1 = 60°F$

Since heat is being transferred out of the system, the water temperature must exceed the shell temperature. Thus, even under the most pessimistic assumptions, temperature control will be maintained when minimum ambient conditions are experienced. If less conservative assumptions are made, it is conceivable that the active cooling system may be required even during minimum ambient conditions. Under this condition, the control temperature could probably be held within ± 2°F tolerance.

8. Pre-Launch Heating Rate

The pre-launch condition must be handled as a special case, because evaporative cooling will not be available. In addition, convective heating will be present at this time. When this heat load is combined with the internal and external heat loads mentioned previously, it is obvious that pre-refrigeration of the experiment will be necessary to limit the temperature of the life-support water supply at lift-off. If this is done, passive thermal control can be achieved. A detailed discussion of the analysis associated with this problem is beyond the intent of this report. It is possible to describe briefly how the convective, conductive, and radiative heating rates can be combined in order to provide a basis for determining the amount of refrigeration that will be required.

A method for determining free convective heating rates from cylindrical and flat surfaces is outlined in Ref. 10. When preliminary calculations were carried out, it became obvious that it would be advantageous if the conductive, radiative, and convective heating rates could be combined into a single expression. This technique was developed, using the experimental data obtained from the engineering model thermal vacuum tests. An expression for an overall heat leakage coefficient is shown below.

$$q_{net} = h_c A(T_1 - T_2) + F_e \sigma A(T_1^4 - T_2^4) + \frac{(T_1 - T_2)}{R} = UA(T_1 - T_2)$$

h_c = free convection heat transfer coefficient, Btu/hr ft^2°F

A = area of pressure vessel

F_e = emittance coefficient

T_1 = temperature of pressure vessel

T_2 = temperature of air and surrounding structure

R = thermal resistance of vibration isolators

U = overall atmospheric heat transfer coefficient, $w/ft^2°F$

Results of the engineering model test indicate that:

$U = 0.17\ w/ft^2\ °F$ for $\Delta T = 30°F$

With the coefficient determined experimentally, a numerical technique can be applied to determine the response of the experiment to the varying heat load. At present, it is felt that sufficient cooling is available to guarantee passive thermal control to lift-off, when the active control system becomes operable. Because of a time lag associated with the installation procedure, experimental data for determining U are not available for temperatures below 55°F. If installation temperatures below this are required, the expected increase in U may require the use of thermal insulation. This factor has been considered in the detailed analysis of the pre-launch condition.

9. Launch Heat Load

The temperatures encountered in the launch phase are outlined in Section II. The rate of heating by radiation leakage will rise to a maximum about 15 minutes after lift-off, but will be reduced to essentially the nominal ambient value in about one hour. The maximum radiative leakage rate at T_{SM} = 130°F is about 19 watts for a shell temperature of 65°F. The excess cooling available with a 5 cc/min evaporator flow rate will be more than enough to overcome this rate. In addition, the air in the Service Module area will be expanding as pressure is reduced, thereby eliminating convective heating almost immediately after lift-off.

VI. SUMMARY OF TESTS (COMPONENT LEVEL)

1. Heat Exchanger

The life-support water is circulated by a pump mounted on the lower bulkhead of the inner assembly. Rotary seals are employed in order to circulate the water to the centrifuge cylinder which encloses the two frogs. About 95% of the water is contained in the cylinder, which is thermally isolated from the upper and lower bulkheads by means of the spin bearings. Although free convection is virtually eliminated in a zero gravity condition, there must be some means of removing the metabolic heat from this water in addition to any that might be radiated to the cylinder from the heat dissipators on the bulkheads. It can also be seen that for any cooling technique that is employed, there must be a relatively quick thermal response of the water system to provide the temperature control required by the experiments.

To satisfy this requirement, it was decided that one sector of the lower bulkhead should be set aside as a heat transfer surface. A pie-shaped plate (Fig. 8) was milled out to provide channelled flow of the life-support water over the surface of a 60° sector of the lower bulkhead. Although analytical calculations were carried out to determine what sort of heat transfer coefficient might be expected, it was decided that the best method of evaluating this unique "heat exchanger" was to set up a laboratory test in which a number of variables could be studied. The machined plate was attached to another aluminum plate which had the same thickness as the lower bulkhead. The outer edge of the plate was clamped between two laboratory cold trap plates. The cold trap

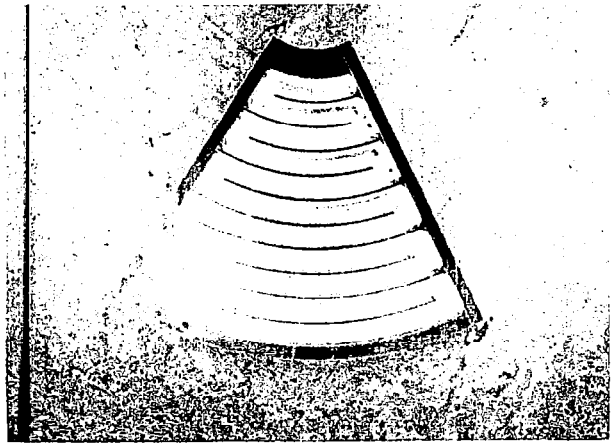

Fig. 8 HEAT EXCHANGER PLATE

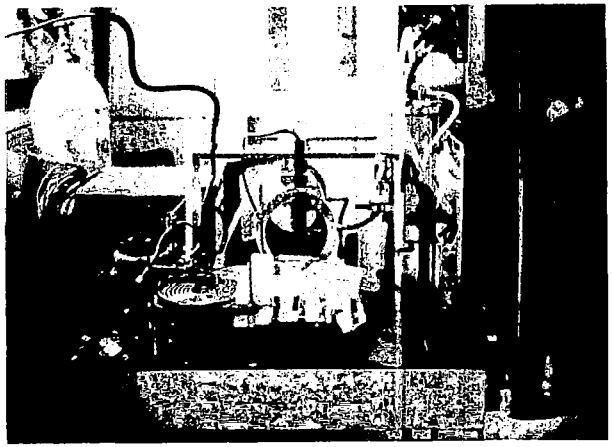

Fig. 9 HEAT EXCHANGER COLD SINK

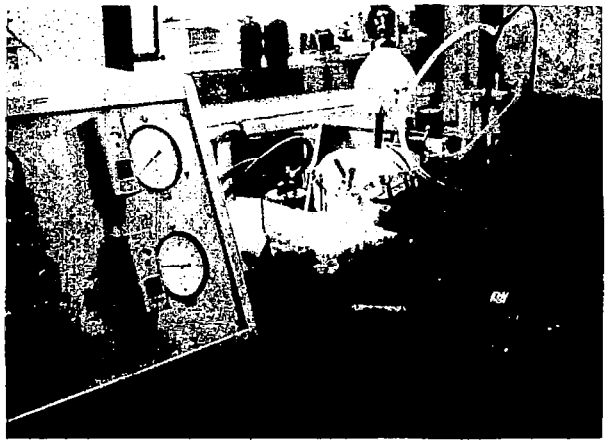

Fig. 10 TEST SETUP FOR HEAT EXCHANGER

was connected to a refrigeration unit to allow circulation of a controlled-temperature fluid through the copper coils (Figs. 9 and 10). The heat exchanger inlet and outlet were connected into a typical life-support circuit which included a pump, General Electric lung, CO_2 cannister, and mock-up centrifuge. The centrifuge cylinder and the heat exchanger were insulated with one inch of non-rigid polyurethane foam.

Temperatures of the various components were recorded. A typical plot of temperature of the water in the centrifuge cylinder is shown in Fig. 11. It is interesting to note the quick temperature response of the water supply as active cooling was initiated. During the test program, it was possible to study the effects of the following variables:

heat sink temperatures
heat load
water flow rate
heat sink contact area.

A calculation procedure was developed to evaluate the net cooling effect of the exchanger. The slope of the water temperature curve was determined during heating and cooling, and the two combined to determine convection losses, which would otherwise have caused erroneous results. The final series of tests was run after modification of the method of clamping the plate into the cold trap. The contact area was reduced to the area provided by the 60° sector of the pressure vessel mounting ring. Fiberglas insulators were employed to provide thermal resistance to the upper cold trap plate, while indium foil was used at the lower plate to reduce contact resistance. The test summary below indicates the relative performance of the experimental heat exchanger.

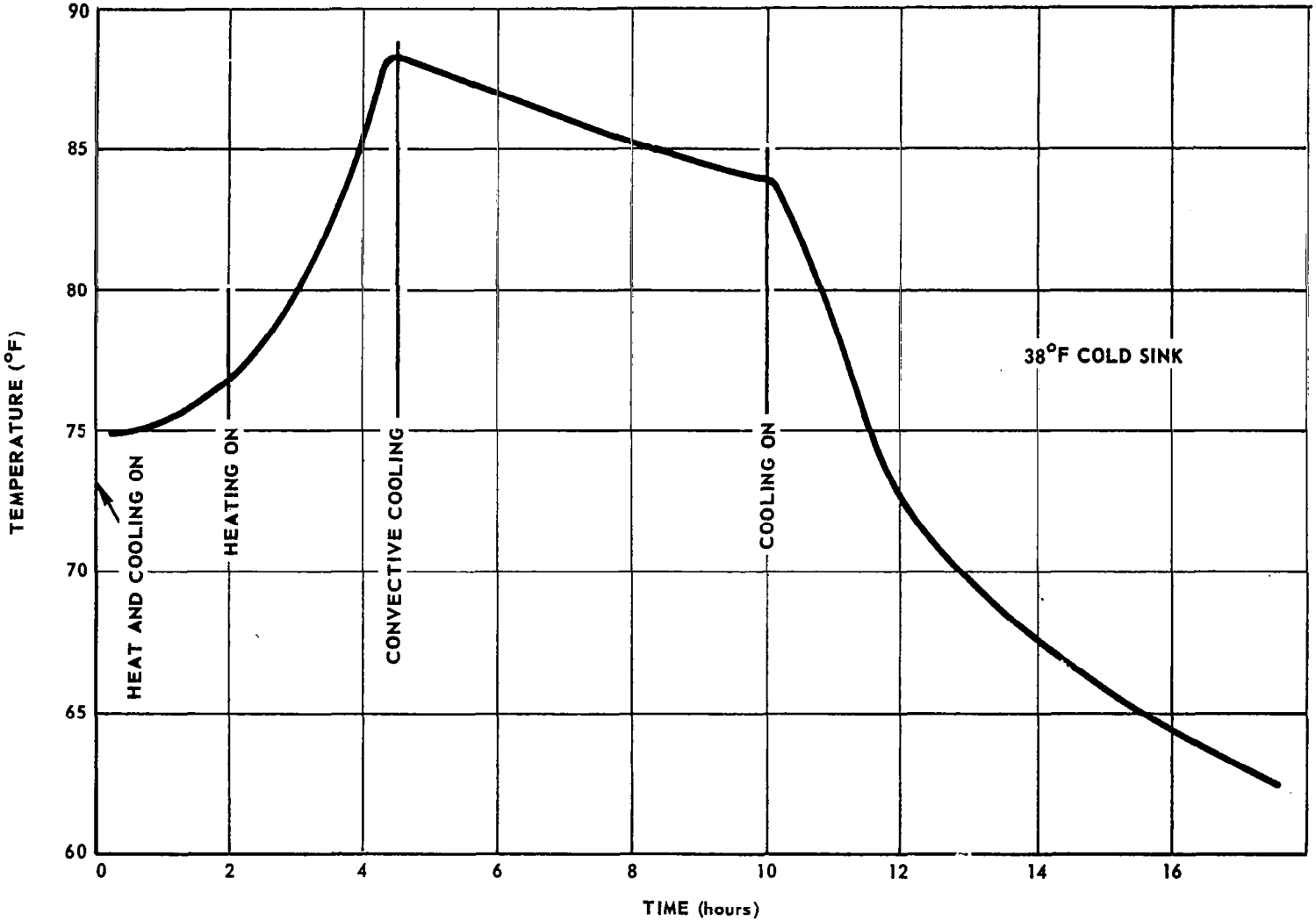

Fig. 11 TEST OF HEAT EXCHANGER, WATER TEMPERATURE VERSUS TIME

No.	Flow Rate	Cold Sink (°F)	T_{calc} (°F)	q_{heat} (w)	$q_{cooling}$ (w)
1	0.21	74°	88°	22.6	13.1
2	0.23	28°	82°	25.2	26.8
3	0.23	38°	83°	24	22.9
4	0.14	38°	71°	24	13.2
5	0.14	38°	71°	22.8	19.8
6*	0.17	38°	82°	22.8	19.9

*Test results for 60° contact area.

Where flow rate = flow rate in life-support water supply, gal/min.

cold sink = temperature of cold trap to which heat was transferred, °F.

T_{calc} = temperature of water at which net cooling was evaluated, °F.

q_{heat} = electrical heat load into centrifuge water supply, w.

$q_{cooling}$ = net cooling effect provided by heat exchanger, w.

The results of these tests have been helpful in refining the analysis procedure developed to study the performance of the heat exchanger in the engineering model system.

Although it may have been possible to improve the heat transfer characteristics by a reduction in channel cross section (i.e., reducing the thickness of the milled-out plate), it was decided that adequate cooling had already been achieved. There was a parallel effort on the part of the mechanical designers to try to minimize drag in the water circuit wherever possible. Obviously, any decrease in flow cross section

would have resulted in a drag increase. Following the completion of the experimental test program, an almost identical exchanger plate was fabricated and later installed in the engineering model.

2. Life-Support Tests

A brief description will now be given of the temperature control system that was assembled for a series of life-support tests which took place at APL in August 1965. The purpose of these tests was to determine the ability of frogs to live at a number of different temperature levels with oxygen supplied by a prototype General Electric lung. Once the tests were completed, the final control temperature of 65 ±5°F was agreed upon.

In order to provide ±1.5°F tolerance on the water temperature, the laboratory model heat exchanger was clamped between two cold plates as shown in Fig. 12. The exchanger was then connected into the life-support circuit and insulated as shown in Fig. 13.

A Honeywell temperature controller was installed, and a thermocouple in the water tank was used to control the flow to the cold trap. With the system in operation, the desired control temperature could be set and maintained for periods in excess of four days. Operation of the system further substantiated the type of response which could be achieved by the use of the heat exchanger.

3. Evaporator

The use of evaporative cooling for a relatively short-term space mission is by no means a new concept; it has been successfully employed

Fig. 12 HEAT EXCHANGER INSTALLATION FOR LIFE-SUPPORT TEST

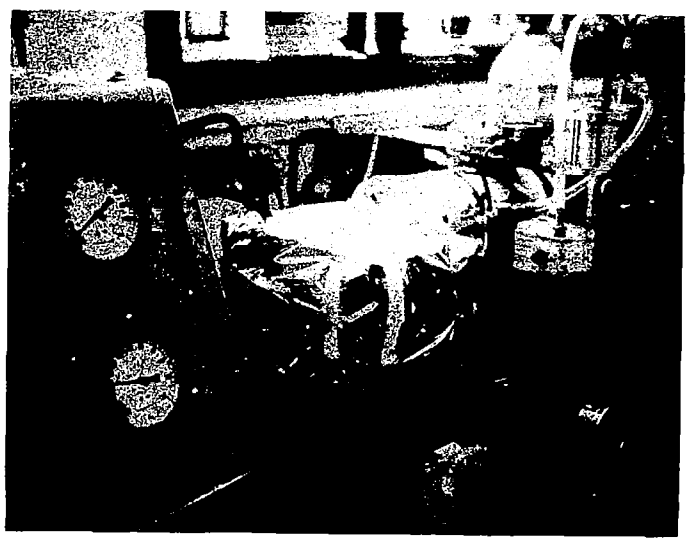

Fig. 13 EQUIPMENT SETUP FOR LIFE-SUPPORT TEST

in the Mercury (Ref. 11) and Gemini Programs, and has been integrated into the suit temperature control system for the Apollo Program (Ref. 12). In each of these instances, the evaporator forms the cold side of a gas-flow heat exchanger. In the otolith experiment, the use of forced convective cooling of the capsule air would be impractical, and thus a different concept had to be devised.

When it was decided to try to provide evaporative cooling, a major part of the mechanical design had been completed. It was therefore decided that, if possible, the evaporator should be integrated into the aft end of the pressure vessel. The basic concept was to provide a chamber which could be maintained at some low absolute pressure. Water, when supplied to the chamber, would expand to this much lower vapor pressure, with an accompanying drop in temperature. A plot of this expansion is shown in Fig. 14. The expanded vapor can be described as 3% quality steam at about 37°F. The cooling capacity is defined as the difference between the enthalpy of saturated steam at 3 in. of water, and the enthalpy at 3% quality at the same pressure. This value has been conservatively rounded off to 1000 Btu/lb. The evaporator pressure is maintained at 3 in. of water by means of a relief valve, in order to prevent freezing at the water inlet. A sketch of the engineering model evaporator is shown in Fig. 15. The evaporator volume is an annulus formed by the domed pressure-vessel head and the evaporator pan. It should be noted that, although the pan is attached by screws to the pressure vessel, an indium foil gasket is used to minimize the thermal resistance of the joint. The 37°F vapor impinges on the dome and pan surfaces, which will normally be at temperatures near 65°F when the evaporator is first turned on.

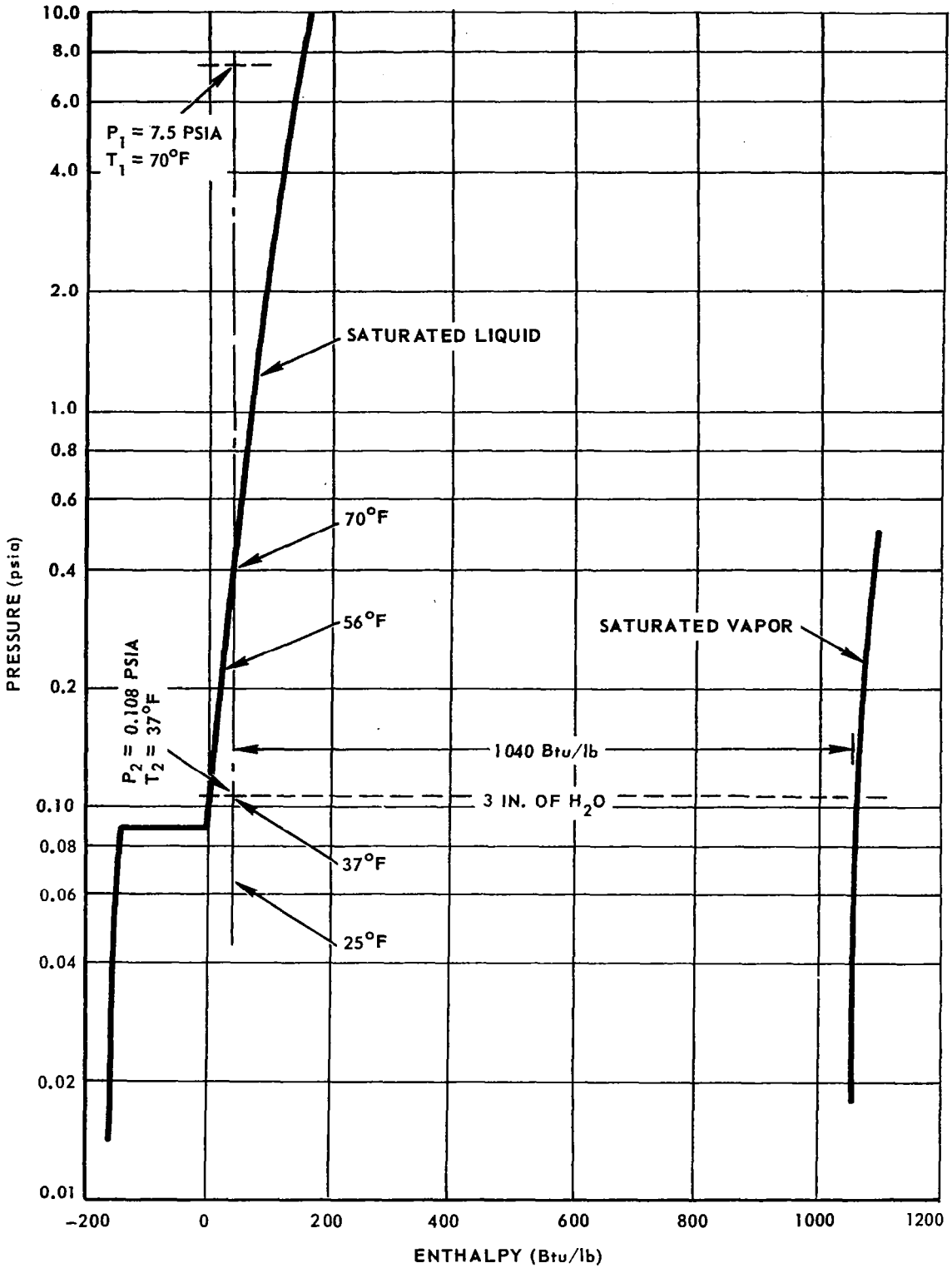

Fig. 14 PRESSURE VERSUS ENTHALPY FOR WATER AT LOW PRESSURE

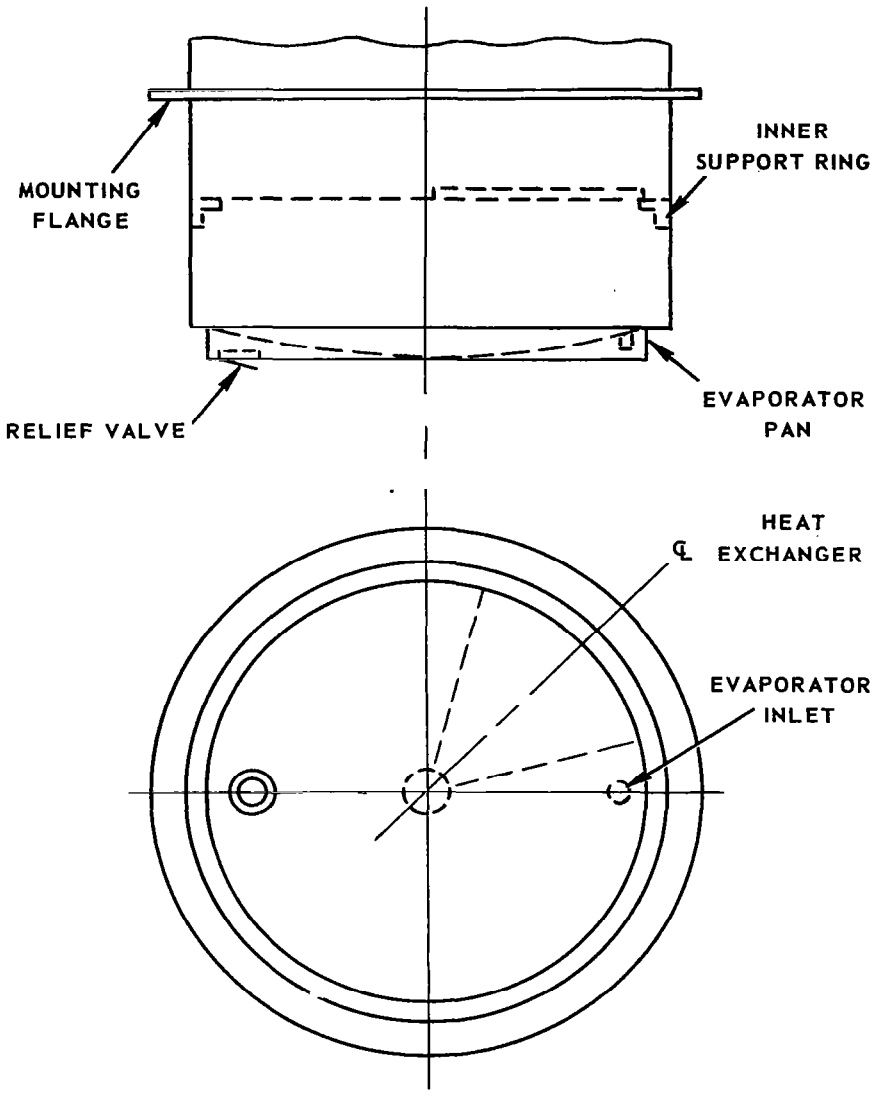

Fig. 15 SKETCH OF THE ENGINEERING MODEL OF THE EVAPORATOR

In this process heat is removed from the system to vaporize the water droplets. The exhaust is steam of nearly 100% quality.

The use of the relief valve also has another advantage. Since a vacuum only slightly better than 3 in. of water is required to produce the desired evaporation, the evaporator can be tested without resorting to the high vacuum of outer space. As a result, most of the early tests on the mock-up evaporator were run at about 150 μ as provided by a roughing pump. This eliminated the risk involved in using the diffusion pumps to reach high vacuum. If diffusion pump oil becomes contaminated with water, a rather troublesome pump overhaul may be required. As experience was gained, however, techniques were developed to trap the steam. Thus, the entire engineering model could be tested under high vacuum conditions without resorting to a separate evaporator pumping system, as was the case in the Mercury Program (Ref. 12).

In order to try to determine such parameters as flow rate, cooling capacity, efficiency, etc., a mock-up was built and tested. The engineering model design was kept flexible so that any improvements which might result from the mock-up tests could be incorporated. Figures 16, 17, 18, and 19 show these tests. As can be seen, some of the tests were run under atmospheric conditions with only the exhaust connected into the vacuum system. This method offered the distinct advantage of ease of assembly, as well as providing the capability of observing the inlet area through a Plexiglas window. Water from a constant pressure supply was metered by a micrometer flow valve, and switched on and off by a solenoid. The system is shown being tested with the relief valve operating against gravity. Other tests were run with the valve in the inverted position, to study the effect of gravity

Fig. 16 TEST SETUP FOR PROTOTYPE EVAPORATOR

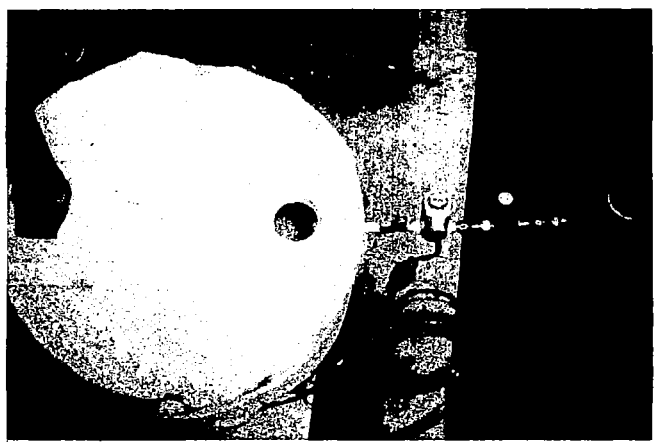

Fig. 17 OBSERVATION PORT, EVAPORATOR INLET

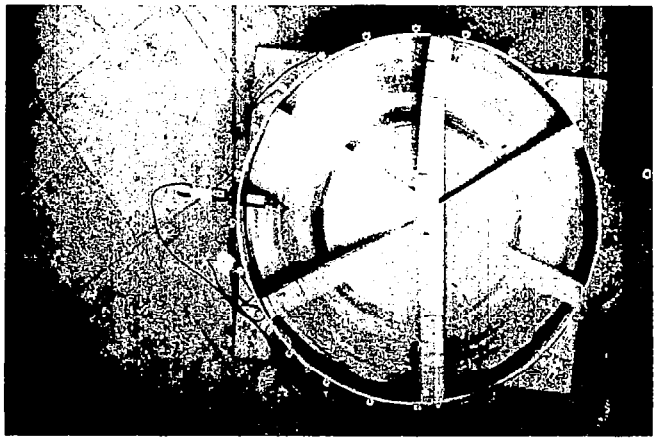

Fig. 18 EVAPORATOR FIN TEST

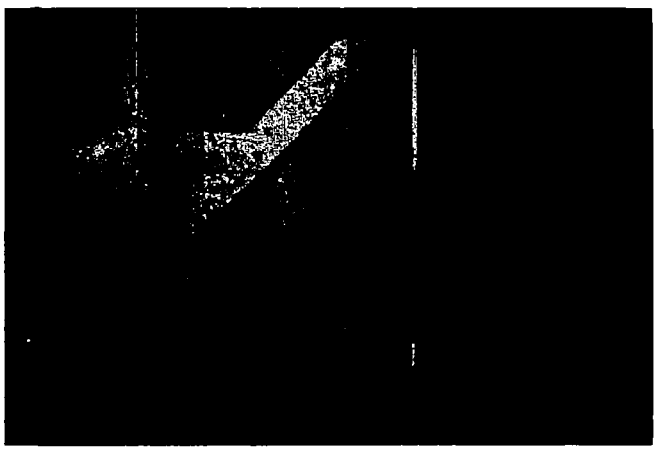

Fig. 19 ICE BUILDUP WITH RELIEF VALVE REMOVED

on the performance of the relief valve. As might be expected, evaporator temperature was about one or two degrees lower with gravity acting with the valve. Because the difference was so slight, it was unnecessary to consider mounting the valve on its side during the one-g system environmental tests.

Once the effect of gravity had been evaluated, a series of tests was run to try to optimize the evaporator design. Among the factors studied were:

1. The effect of the orifice size at the inlet
2. The effect of flow rate, as adjusted by the micrometer valve
3. The effect of radial honeycomb fins to increase heat transfer surface (Fig. 18)
4. The linearity of flow rate with time, and the repeatability of flow rate
5. The performance of the torsion spring "flapper" valve, as compared with a compression spring disk valve.

A method was developed to determine the efficiency of a given test condition. A group of thermocouples was distributed on the surface of the mock-up, which was then insulated with one inch of non-rigid polyurethane foam. After a test run, the record was examined to determine the average drop of the mock-up's thermal inertia. An efficiency was then determined as shown below.

$$\varphi = \frac{W_e C_e \Delta T}{W_{H_2O}(1000)}$$

φ = efficiency

W_e = total weight of mock-up

C_e = specific heat of mock-up

W_{H_2O} = weight of water used during test run

ΔT = drop in temperature of mock-up

It was possible to determine graphically the convective heating of the system where more accurate information was desired. As a result of the test program, it was decided that the aircraft "flapper" valve would be used in the system and that radial fins would not be needed. Under controlled conditions, it was possible to achieve φ values > 90% for the system.

As a matter of interest, a test run was made without a relief valve in the system. The photograph (Fig. 19) on page 43 shows quite dramatically how such a system freezes up with a resulting stoppage in coolant flow.

As previously stated, the mock-up evaporator included a micrometer flow valve to provide for flow adjustment. Although it provided a mechanical means of metering flow, the solenoid was a continuous drain on the power system. During the mock-up tests, it was possible to control flow down to as low as 1.5 cc/min, but no test runs were made beyond 30 min of continuous flow. During thermal vacuum tests of the engineering model, a problem developed which has resulted in the elimination of the micrometer valve in favor of an electronic timing circuit. Although this problem will be discussed in the next section, a brief description will now be given of the flow rate tests which were carried out to eliminate the problem of diminishing flow rate.

During the engineering model tests, the evaporator remained "on" for periods as long as four hours. However, at the completion of such a test, only about 400 cc of water had been removed from the bladder.

To better define this problem, a series of tests was run using time as the only variable. Test results showed a series reduction in flow rate for periods beyond 30 min. There was no obvious reason for the reduction. A laboratory test was set up to evaluate the bladder by measuring flow rate with the bladder upright and inverted. The evaporator inlet was connected to a 7.5 psia chamber in order to provide the necessary differential pressure (Fig. 20). Although the effect of gravity was noticeable, the flow was linear for each case. Under high vacuum conditions (Fig. 21), however, flow beyond 30 min was accompanied by a gradual decrease in the rate of change of internal pressure in the pressure vessel. Since the micrometer valve provided the greatest restriction to flow, it was decided that the valve should be removed and additional metering supplied by a timing circuit. Test results indicate that the system will provide uniform flow even for extended time periods. Pressure monitoring during this type of flow shows a linear decrease in internal pressure, as expected for linear water flow.

In concluding this section on the evaporator, it should be noted that during the final flow tests it was possible to observe the "flapper" valve by means of a mirror, and that any fear of a frost build-up as the steam hit the high vacuum was dispelled (Fig. 21).

Fig. 20 LABORATORY FLOW TEST OF THE EVAPORATOR

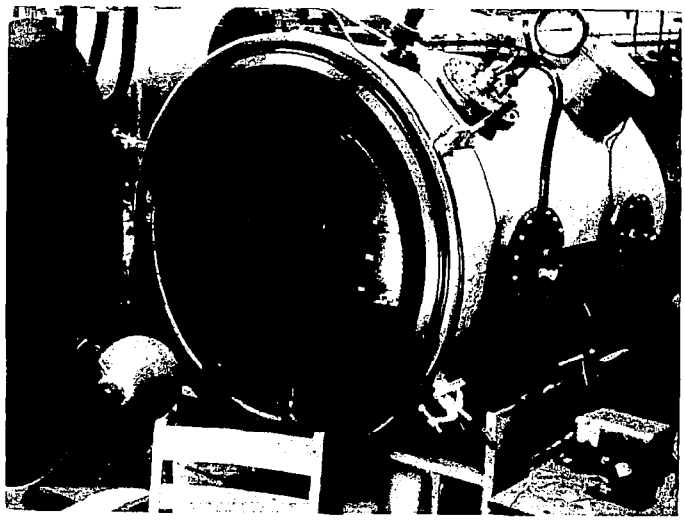

Fig. 21 FLOW TEST OF THE EVAPORATOR IN THE VACUUM CHAMBER

VII. THERMAL VACUUM TESTS OF ENGINEERING MODEL

Prior to receiving NASA approval to initiate the flight prototype phase, a series of environmental tests was run to evaluate the performance of the engineering model. The system thermal vacuum test program will now be described, along with the test results. A thermal vacuum test procedure was developed which can be employed, with minor changes, in the testing of the flight prototype and flight models. NASA requested that the model be subjected to specification temperature levels for all three phases of the mission. Tests were to be long enough to prove the adequacy of the temperature control system as well as to evaluate the performance of the entire experiment under flight conditions.

1. Test Equipment and Procedure

In order to carry out the test program, a structure was built to simulate the mounting platform and surrounding structure of the Service Module. For obvious reasons, the geometry of the Bay I section could not be completely duplicated. The geometric relationship between the beam and the vertical axis of the outer shell was preserved. A photograph of the simulator (which is roughly four feet in overall height) is shown in Fig. 22. The plastic hose visible in the photograph is connected to a fitting at the relief valve location in order to channel evaporator exhaust to the cold trap shown in Fig. 23.

Fig. 22 SERVICE MODULE SIMULATOR

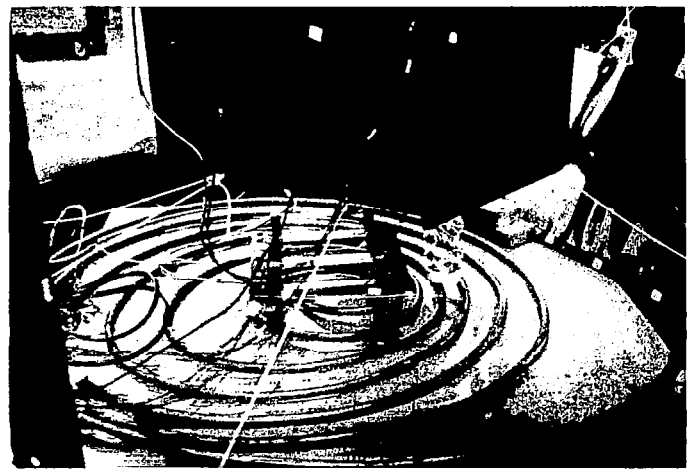

Fig. 23 VACUUM CHAMBER COLD TRAP

Temperature control of the simulator is acheived by means of cold vacuum-chamber walls and a set of quartz lamps. Four separate temperature controllers are used in conjunction with the lights to set the temperatures required in the specification. A total of 12 calibrated thermocouples are mounted on the surface of the simulator and six more are mounted on the honeycomb deck. The vibration isolator ring is installed in order to provide a good simulation of the conductive thermal resistance. The outside of the simulator is painted black to improve the temperature control capability. The internal surfaces are painted with H and H Silpaint 2060-01, which has a measured infrared emittance very close to the 0.25 indicated by NAA. A plot of experimental simulator temperatures is shown (Fig. 24) to give an indication of the type of control that has been achieved. It should be noted that the shelf temperatures are controlled passively and follow the outer structure temperatures very closely. Since a considerable amount of thermal resistance is built into the vibration isolator ring, it is felt that a more accurate simulation of the shelf temperature is not required.

Although the plots in Fig. 7 indicate that the post-launch temperature decay will take about five hours to stabilize, it is possible to get a good approximation of the decay by employing a linear decay of about 1-1/4 hr duration. Once the steady state ambient is set, it can be controlled indefinitely. In order to change from the maximum (80°F) to the minimum (40°F) steady state ambient, the controls can be set manually at any ramp rate desired. As shown in the graph, this change-over time can be as short as fifteen minutes.

The pre-launch phase test is also carried out in the Service Module Simulator. The vacuum chamber door is raised into position and held there, without benefit of vacuum, by a hydraulic lift. Wall temperature

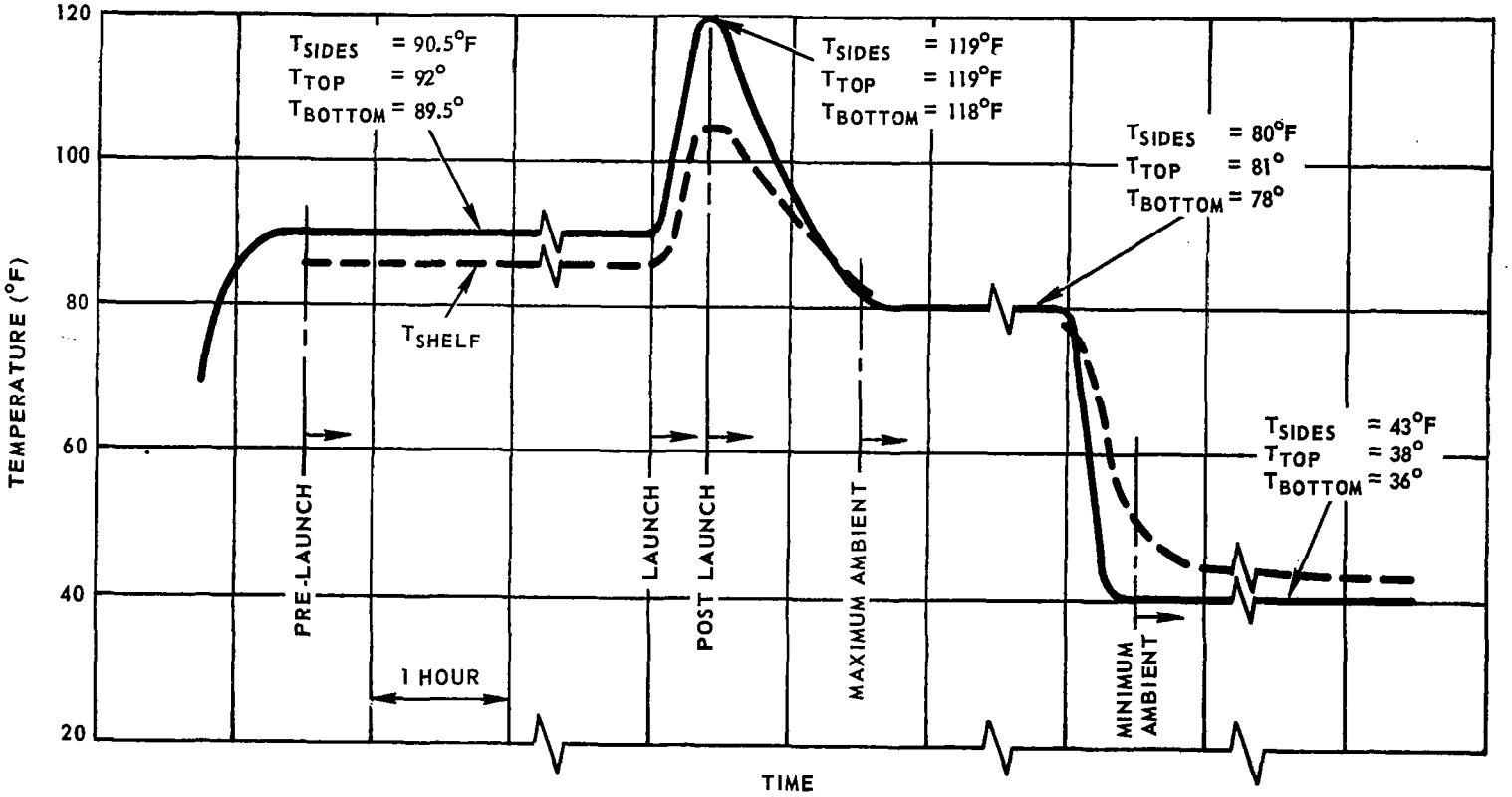

Fig. 24 TEMPERATURE CONTROL OF THE SERVICE MODULE SIMULATOR

can then be controlled with relatively low voltage so that it is not necessary to have cold walls for this portion of the test. As a result, the air in the simulator is in a near stagnant condition, thus providing a relatively good simulation of the pre-launch phase. In order to provide a close simulation of the launch temperature profile and to collect any evaporator exhaust, the chamber walls are chilled with liquid nitrogen just after the vacuum hot-rough is started.

It was previously mentioned that a cold trap has been built which should collect the evaporated steam. Liquid nitrogen is circulated through the copper coil. In the first attempt at trap design, the coil was sandwiched between two large flat plates, with the plastic hose inlet near the center. The system appeared to work satisfactorily until pressure began building up in the evaporator. The problem was diagnosed as a frost blockage, and as a result the upper plate was removed. This change also made it possible to mount a piece of reflecting Alzak in such a way that the evaporator exhaust and frost build-up could be observed through one of the vacuum chamber port holes. After a satisfactory cold trap was developed, it was possible to maintain the vacuum at 2×10^{-5} mm of Hg during evaporator operation.

The Service Module Simulator has been mounted on one of the spare doors of the large vertical vacuum chambers. This door has the cold trap built-in, a permanent light ring to control sidepanel temperatures, and separate banks of lights to control the top and bottom surface temperatures. Sixty-four thermocouples can be fed through the door, in addition to signal and test cables. In the engineering model, it was possible to install nine thermocouples inside the pressure vessel by replacing the 19-pin signal plug. These couples were used to record the temperatures of the following items:

1. Heat exchanger inlet
2. G. E. lung
3. Pump motor
4. Blower motor
5. CO_2 absorber
6. Inner assembly support ring (at heat exchanger)
7. Upper bulkhead (inverter)
8. Thermostat mount
9. Evaporator water supply lid

In addition to the thermocouples for the simulator and the internal experiment, the pressure vessel was instrumented with 30 additional thermocouples. Once the general response of the shell had been established, it was possible to reduce the number of external thermocouples thereby cutting down installation time. The assembly procedure is outlined below.

1. Final assembly of inner assembly and sealing of pressure vessel lid
2. Mounting of experiment in simulator and connection of test cables
3. Location of the pressure vessel thermocouples, including one inside the plastic tube at the relief valve
4. Mounting of simulator front panel and attachment of front panel thermocouples
5. Checking for continuity of all thermocouples through chamber door
6. Connection of temperature recorders to provide continuous recording of up to 64 temperatures

7. Connection of control thermocouples to temperature controllers and checking lights for proper performance
8. Raising of chamber door to initiate test

Several photographs are included (Figs. 25, 26, 27) to show the system in the final stages of preparation, and finally, the monitoring station while a test is in operation.

2. Test Results

The thermal vacuum test of the engineering model was completed during a three-week period in October 1965. The final test in the series was observed by the experimenter and by NASA representatives from the Ames Research Center and the Manned Spacecraft Center, Houston, Texas. The initial phase of the program was used not only for preliminary evaluation of the experiment, but also to evaluate and improve the test facility and procedure. The results of the program are listed below.

1. The Pre-Launch Condition was simulated on two occasions. Data have been used to determine pre-flight control design limits. The chamber simulation is good and temperature control is accurate.
2. The Launch Phase was simulated on two occasions. The temperature control of the simulator is extremely flexible. Manual control of temperature rise and decay has been worked out for future test programs. The experimental thermal inertia is large enough to minimize the effect of higher temperatures which accompany this phase.

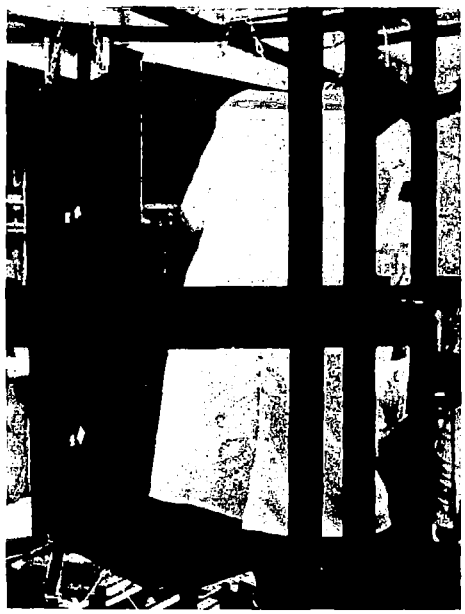

Fig. 25 INSTALLING THE EXPERIMENT

Fig. 26 VACUUM CHAMBER ASSEMBLY

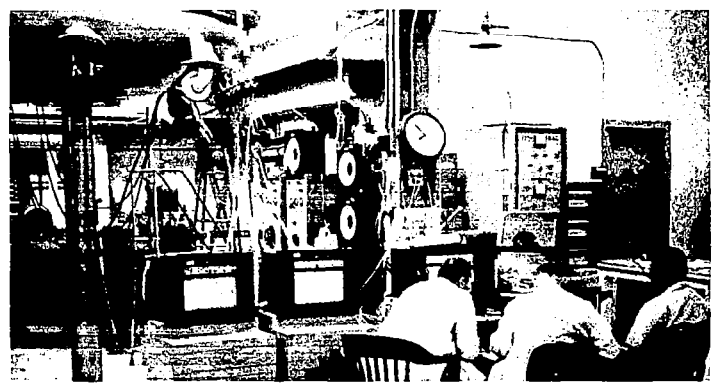

Fig. 27 MONITORING STATION FOR THERMAL VACUUM TESTS

3. The Maximum Structural Ambient Condition was simulated on a number of occasions. During the final two tests, the on-off duty cycle of the evaporative cooler operated successfully despite a problem with coolant flow rate. This problem has since been eliminated. Control of simulator temperatures as well as the cold trap design have been successfully worked out for the flight prototype test program.
4. The Minimum Structural Ambient Condition was carried out to the steady-state condition. Final control temperature stabilized within the temperature tolerance.

A number of the experimental temperature plots will now be presented along with a brief discussion to clarify some of the points mentioned in the outline of the results. In view of the fact that there was some delay and considerable handling before the plated pressure vessel was polished, it was felt that the emittance of the coating was higher than originally expected. For example, a change in infrared reflectance from 95% to 80% would increase the emittance by a factor of four. Thus, it was decided that the original NAA temperature limits should be used in the simulation. This decision was altered for the test performed for the NASA representatives and a noticeable change in performance was observed. A coating specification has been drawn up to ensure that the proper emittance will be achieved on the flight vessels.

The pre-launch phase tests were less than completely successful. This was to be expected, however, in view of the fact that a key part of this phase is the assembly procedure. Although refrigeration techniques were employed, there were considerable delays imposed by a number of factors. Primary among these factors was the time spent in readying

the experiment once it had been installed in the Service Module Simulator. In order to derive the desired amount of temperature information, some 30 thermocouples had to be located and installed. Without going into detail, it has been possible to use the experimental results to ensure proper temperature control under the preflight conditions. Figure 28 gives a plot of average water temperature for one of the early tests.

As stated earlier, the launch and post-launch temperature-decay conditions pose no serious problems. Successful operation of the evaporator was observed as soon as vacuum conditions were reached, on those occasions when the water temperature had risen above 65°F prior to simulated lift-off. In view of the fact that cold chamber walls provide a high rate of convective cooling when there is air in the chamber, it has been necessary to initiate vacuum pumping before chilling the tank walls. Because a rough vacuum is reached relatively quickly, it is possible to initiate liquid nitrogen flow soon enough to prevent any problem due to evaporation during the launch simulation. The procedure has been successfully worked out by Robert Pollack, of the Environmental Test Laboratory (ETL), who was also responsible for the design and fabrication of the cold trap.

Operation of the evaporative cooler was impaired by a number of factors, two of which were eliminated during the test program. One of the early problems was the frost buildup in the cold trap. This phenomenon was relatively difficult to uncover, but once the trap design was altered, the system functioned without a pressure buildup in the evaporator. The second factor resulted from the attempt to provide for coolant metering by means of a mechanical micrometer valve. In order to provide for the relatively low flow rate, the valve had to be closed to such a small

opening that inconsistent performance was experienced. In addition, this method required that the solenoid be "on" continuously during evaporation. This resulted in a continuous 7.8-watt load which seriously impaired the overall efficiency of the system. As a result, it was decided that the solenoid would be controlled by an electronic timer. This not only resulted in a reduced continuous electric load but also made it possible to adjust the micrometer valve to a more open position. Since the timer was an afterthought, it was decided that it would be advisable to employ the circuit external to the vacuum chamber so that the duty cycle of the timer could be changed in order to adjust coolant flow. A third factor, that of flow decay with time, has since been eliminated by removal of the micrometer metering valve.

Although not stated previously, the temperature of the life-support water supply will be monitored by means of a thermistor bridge circuit in order to provide the experimenter with a reference temperature record. The original design concept had the thermistors mounted inside the centrifuge cylinder. This has since been changed because of a leakage problem, but it was possible to get a good experimental correlation of thermistor temperature measurements versus the thermocouple measurements of other temperatures in the water circuit, such as the heat exchanger and thermostat temperatures (Fig. 29).

It was stated earlier that during the final two tests observation of the on-off duty cycle of the evaporative cooler provided proof that the design concept is feasible, and can be made quite precise. Under each condition the experiment was installed and subjected to the maximum ambient condition. Since only the steady-state control was being evaluated, the evaporator was not turned on until high vacuum conditions

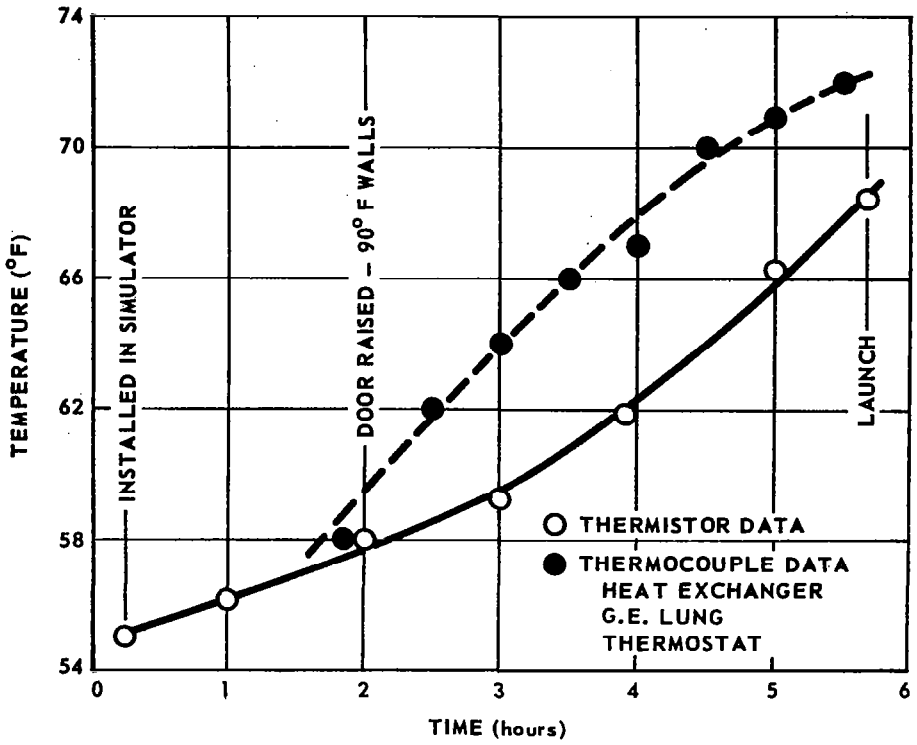

Fig. 28 PRELAUNCH PHASE, AVERAGE WATER TEMPERATURE VERSUS TIME

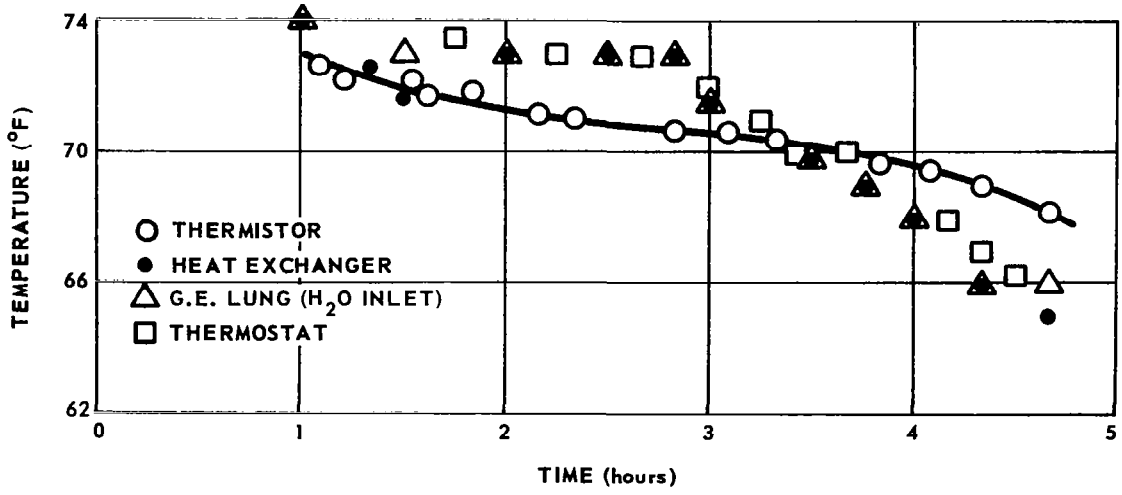

Fig. 29 THERMISTOR DATA VERSUS THERMOCOUPLE DATA

were reached. Once the evaporator was turned on, cooling was initiated. The system was then monitored to determine the "on" and "off" times.

On 29 October 1965, an evaporator "on" time of approximately 2.5 hr was recorded, followed by an "off" time of approximately three hr and 40 min. There was extremely good correlation between the temperature data and the thermostat, which had been set for 65°F. After the evaporator had been turned back on as the 65°F temperature was reached, it was decided that the test plan should be altered to include a test at minimum ambient temperature condition.

The test was then continued with the simulator walls set at 40°F until it appeared that a steady-state temperature condition had been reached. At this point, the average temperature of the water supply had stabilized at 60.5°F. The test lasted a total of about 10 hours; a plot is shown in Fig. 30. Although the "off" time (in excess of 3 hr) looked extremely good, there was obviously some problem associated with evaporator flow. An "on" time of 2.5 hr should have permitted the flow of approximately 750 cc of water, but when the weight of the water supply was checked, it was found that only about 400 cc had been evaporated. It can be shown that the evaporator operated efficiently on its reduced supply, but there was no immediate explanation of the reduced flow.

Before the flow problem could be completely analyzed and eliminated, it became necessary to run another thermal vacuum test for the NASA visitors. This second successful run was carried out on 2 November 1965. Without going into detail, a "on" time of about four hours was experienced, most of which was spent with the 90°F simulator walls requested by NASA. The system "off" time of 2.7 hr was somewhat

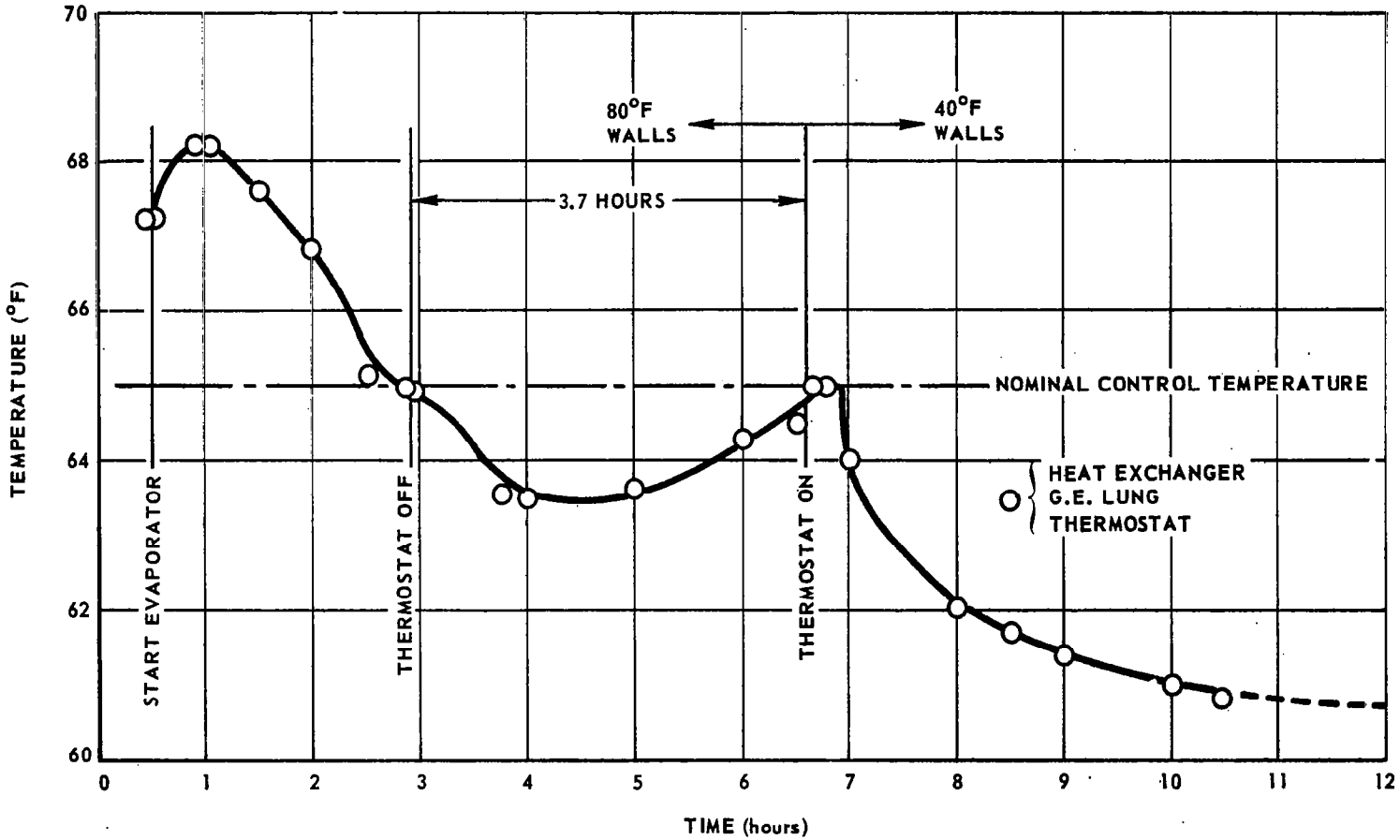

Fig. 30 RESULTS OF THERMAL VACUUM TEST; WATER TEMPERATURE VERSUS TIME

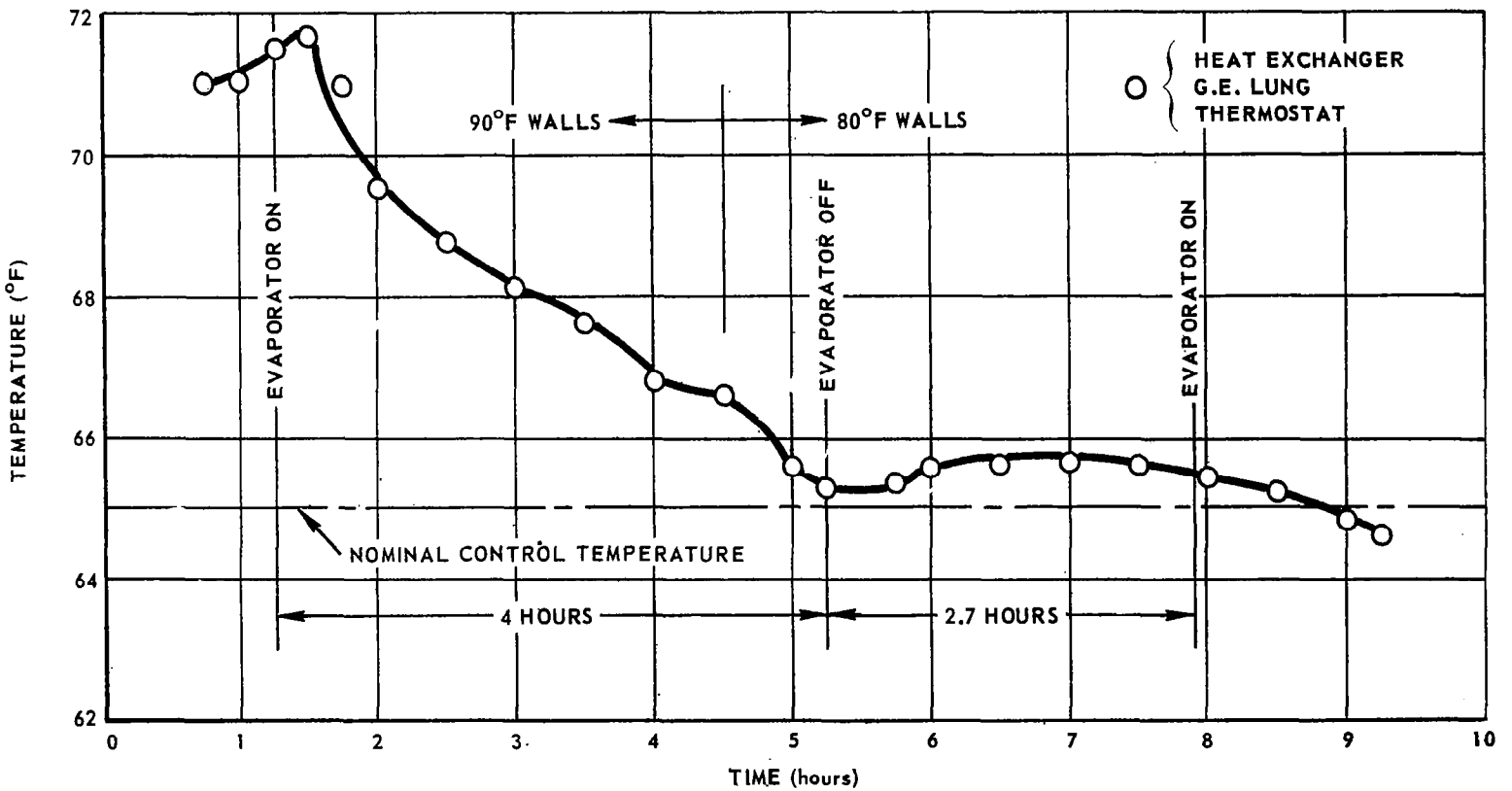

Fig. 31 RESULTS OF THERMAL VACUUM TEST, WATER TEMPERATURE VERSUS TIME

shorter, probably because of the increased heat stored in the upper half of the shell. A plot is shown in Fig. 31. It should be noted that the correlation is somewhat impaired because of a change in temperature recorders for this particular test. At the completion of this test, the coolant usage was again determined and found to be considerably lower than expected. It was at this time that the evaporator flow test program was initiated, and the problem eliminated.

The thermal vacuum tests also served as a good proving ground for tests on the entire system. The lessons learned should result in a well thought-out flight prototype test program.

VIII. CONCLUSIONS AND RECOMMENDATIONS

At the completion of the engineering model phase, it is possible to conclude that a system thermal design has been developed which will meet the requirements set by the experimenter. Most of the problems which affected performance of the thermal control system have been eliminated. There are a number of areas where changes in the life-support system and the thermal control system may be implemented to improve reliability, ease of manufacture, performance, etc. It is recommended that these changes be monitored very closely to determine their effect on the thermal design.

In addition, a number of items are vital to the successful operation of the thermal control system. The most important of these are listed below. They will require careful control in the flight prototype model.

1. External nickel plating
2. Indium foil at the internal support ring
3. Indium foil at the evaporator pan joint
4. Accurate determination of coolant flow rate
5. Determination of an optimum assembly procedure to minimize heat build-up time at the refrigerated condition
6. Continuous internal heat load (electric power dissipation).

Finally, it is recommended that there be a continuing effort to try to obtain any new information that might become available regarding

Service Module changes, pre-launch installation procedures, orbital orientation definition, etc. These results should be evaluated in regard to their effect on the thermal system and hence the overall success of the Orbital Otolith Experiment.

REFERENCES

1. P. R. Schrantz, "Preliminary Design Review of the Thermal Control for the Orbital Otolith Experiment," APL S43-3-8, 24 March 1965.

2. P. C. Merhoff, Temperature Data for Action Item 12-N-20-01 (S-14 Scientific Experiment Package), FS/ATC 65-101, Internal Ltr. of NAA, 12 August 1965.

3. D. Maize, Dept. 696/532 Heat Transfer, NAA, Downey, Calif., telephone communication, 15 March 1965.

4. B. H. Jennings and S. R. Lewis, "Air Conditioning and Refrigeration," 4th ed., International Textbook Co., 1958.

5. APL Ltr. TS-1095, Enclosure (1), Section D, 30 September 1965.

6. E. R. G. Eckert and R. M. Drake, "Heat and Mass Transfer," 2nd ed., McGraw-Hill Book Co., New York, 1959.

7. Honeywell Research Center, "Thermal Radiation Properties Survey," 2nd ed., Minneapolis-Honeywell Regulator Co., 1960.

8. W. D. Wood, H. W. Deem, and C. F. Lucks, "The Emittance of Iron, Nickel, and Cobalt and their Alloys," DMIC Memo 119, Battelle Memorial Institute, July 1961.

9. Howard T. Betz, et al., "Determination of Emissivity and Reflectivity Data on Aircraft Structural Materials," Armour Research Foundation, October 1956.

10. C. L. Strodtman, "Heat Flow Estimation," Electro Technology, March 1965, pp. 83-85.

11. J. A. Maloney and F. G. Richardson, "Tests of a Life Support System Under Simulated Operating Conditions," Proceedings of the National Meeting, 1961, Institute of Environmental Sciences, 1961.

12. W. C. Kincaide, "Space Suit for the Moon," Mechanical Engineering, Vol. 49, November 1965, pp. 49-53.

NASA-Langley, 1967 — 3 CR-815